

Brogioli, Doriano ; La Mantia, Fabio



Innovative technologies for energy production from low temperature heat sources: Critical literature review and thermodynamic analysis

Journal Article as: peer-reviewed accepted version (Postprint)

DOI of this document* (secondary publication): <https://doi.org/10.26092/elib/3659>

Publication date of this document: 14/02/2025

* for better findability or for reliable citation

Recommended Citation (primary publication/Version of Record) incl. DOI:

D. Brogioli and F. La Mantia , Energy Environ. Sci., 2021, 14 (3) , 1057 –1082.
<https://doi.org/10.1039/D0EE02795B>

Please note that the version of this document may differ from the final published version (Version of Record/primary publication) in terms of copy-editing, pagination, publication date and DOI. Please cite the version that you actually used. Before citing, you are also advised to check the publisher's website for any subsequent corrections or retractions (see also <https://retractionwatch.com/>).

This document is made available with all rights reserved.

Take down policy

If you believe that this document or any material on this site infringes copyright, please contact publizieren@suub.uni-bremen.de with full details and we will remove access to the material.

Innovative technologies for energy production from low temperature heat sources: critical literature review and thermodynamic analysis.

Doriano Brogioli and Fabio La Mantia

Universität Bremen, Energiespeicher- und Energiewandlersysteme,
Bibliothekstraße 1, 28359 Bremen, Germany

Abstract

The scientific community has taken on the challenge to develop innovative methods to exploit low-temperature ($<100^{\circ}\text{C}$) heat sources, having a large potential to decrease the carbon footprint. In this review, we first summarise the novel proposed techniques, then we propose a framework for comparing the performances reported in literature based on two indices, which are currently critical for the technical and economical feasibility: energy efficiency and power density. Two techniques show the best performances; both use distillation to regenerate the working solution of a flow battery. In many papers, schemes based on additional heat exchangers are proposed with the aim of improving the efficiency. Such techniques are also discussed here; first, the power per unit surface of heat exchangers is discussed as a performance index; then, a method for inherently ranking the techniques, independently on the use of additional heat exchangers, is provided. The analysis shows that the application of such schemes does not significantly change the ranking of the techniques, while having a detrimental effect on the complexity of the whole system. Finally, we discuss the performances of the various techniques based on general thermodynamic principles and methods; in particular, the meaning of the temperature *versus* entropy graph in this context is considered.

Broader context

A large amount of heat is available from low-temperature ($<100^{\circ}\text{C}$) heat sources, which include renewable and easily accessible sources such as low-concentration solar collector and shallow-well geothermal plants. The exploitation of such sources could be easily decentralised and performed at small scale, with advantages for the flexibility of the power grid. Household heat-and-power

generation (co-generation) and recovery of industrial waste heat would also benefit from the exploitation of low-temperature heat sources. Traditional technologies for the exploitation of low-temperature heat sources are thermal engines and thermoelectric solid-state modules, which are however still not widespread in the market. Thus the scientific community has taken on the challenge to develop innovative methods to exploit the low-temperature heat sources alternative to the traditional technologies. In this review, the innovative methods are discussed. The aim is to provide a uniform framework for a proper comparison of the innovative techniques, based on the performance indices that are most critical for the technical and economical feasibility, and to highlighting the most promising research lines.

Contents

1	Introduction	5
2	Description of the techniques presented in literature	8
2.1	Thermogalvanic cells (TEC)	9
2.2	Electrochemical heat engine (TREC)	10
2.3	Method based on copper-acetonitrile complexation and disproportionation	11
2.4	Method based on ammonia complexation	13
2.5	Thermo-osmosis	15
2.6	Thermal separation - salinity gradient power	16
3	Comparison of the performances	19
3.1	Efficiency	19
3.2	Assumptions on the performances of additional heat exchangers	21
3.3	Power density	21
3.4	Comparison of literature results	22
4	Multi-effect combination and heat recuperation schemes	22
4.1	Multi-effect combination and heat recuperation schemes (MEHRS)	22
4.2	Power density per heat exchanger surface	26
4.3	Trade-off between ρ and η	27
4.4	Intrinsic performance indices ΔT_* and η_*	29
4.5	Approximate expressions for η and ρ	31
5	Technical and economical feasibility	32
5.1	Technology readiness level	32
5.2	Partial evaluation of costs based on p and η	33
5.3	Cost of heat exchangers	34

5.4	Occupation of space and complexity of the system	35
6	Discussion of the techniques based on fundamental physical principles	36
6.1	Thermogalvanic cells (TEC)	36
6.2	Electrochemical heat engine (TREC)	37
6.3	Method based on copper - acetonitrile complexation (CuACN) .	40
6.4	Thermally regenerative ammonia battery (TRAB)	42
6.5	TO	43
6.6	Distillation-salinity gradient power (TS-SGP)	44
6.6.1	Vacuum distillation (VD)	44
6.6.2	Membrane distillation (MD)	48
6.6.3	Thermolysis (TL)	48
7	Conclusion	48

Acronyms

BattMix	Battery mixing
CapMix	Capacitive mixing
CRFB	Concentration redox-flow battery
CuACN	Method based on copper-acetonitrile complexation
MD	Membrane distillation
MEHRS	multi-effect and heat recovery scheme
PEM	Proton-exchange membrane (fuel cell)
PRO	Pressure-retarded osmosis
RED	Reverse electrodialysis
SGP	Salinity gradient power
TEC	Thermoelectrochemical cells = Thermogalvanic cells
TL	Thermolysis
TO	Thermo-osmosis
TRAB	Thermally regenerative ammonia battery
TRB	Thermally rechargeable battery
TREC	Thermally regenerative electrochemical cycle = Electrochemical heat engine
TRL	technology readiness level
TS	Thermal separation
VD	Vacuum distillation

Mathematical symbols

Symbol	Description	unit
c_h	cost per unit power of collected heat	€/W
c_{he}	cost per unit surface of heat exchangers	€/m ²
$c_{he,*}$	single-effect equivalent of c_{he}	€/W
c_s	cost per unit surface of cell	€/m ²
n	number of effects	
p	power density	W/m ²
P	power	W
Q_A	Heat captured in step (A) of a cycle	J
Q_B	Heat captured in step (B) of a cycle	J
Q_H	Heat captured from the heat source	J
Q_L	Heat released to the heat sink	J
Q_{he}	Heat crossing the heat exchangers	J
S	Surface of heat exchangers	m ²
T	Temperature	K
T_H	Temperature of the heat source	K
T_L	Temperature of the heat sink	K
$T_{proc,H}$	Upper temperature of a single process of a MEHRS	K
$T_{proc,L}$	Lower temperature of a single process of a MEHRS	K
U	Heat transfer coefficient	W/(m ² K)
W	Produced work	J
ΔG	Produced free energy	J
ΔT_*	Temperature difference across a single process of a MEHRS	K
ΔT_1	Temperature difference across the heat exchanger in contact with the heat source	K
ΔT_{he}	Temperature difference across a heat exchanger	K
α	Thermoelectric coefficient	V/K
η	Energy efficiency	
η_*	Energy efficiency of a single process of a MEHRS	
η_C	Energy efficiency of the Carnot cycle	
$\eta_{2nd-law}$	2nd-law efficiency η/η_C	
$\eta_{2nd-law,*}$	2nd-law efficiency of a single process in a MEHRS	
η_{EP}	Energy efficiency of electrochemical process	
η_{SGP}	Energy efficiency of SGP process	
η_{TP}	Energy efficiency of a thermal process	
$\eta_{TP,*}$	Energy efficiency of a single thermal process in a MEHRS	
η_{TS}	Energy efficiency of thermal separation	
$\eta_{TS,*}$	Energy efficiency of a single thermal separation process in a MEHRS	
ρ	Heat exchanger specific power, i.e. the power per unit heat exchanger surface	W/m ²

1 Introduction

Developing engines for producing work from heat was the practical application that stimulated the development of thermodynamics in the nineteenth century [1]. Currently the technological level of heat engines is high [2] and complex systems are built for reaching high efficiency [3]. Heat engines are massively used for the production of electrical current from heat generated by burning fuels [4]. In order to decrease the carbon footprint, heat engines have been also applied to the exploitation of renewable heat sources such as solar collectors [5].

The performances of heat engines, often based on Rankine or Brayton cycle, are excellent in large-scale applications but, up to now, they failed to penetrate the market of small-scale applications, at the level of household [6]. The availability of devices for the exploitation of low-temperature heat at small scale would enable a more widespread exploitation of renewable and clean sources and decrease the land footprint; decentralising the energy production is encouraged in general [7] and requires the down-scaling of the energy production technology. Thus, developing small-scale technologies able to work at low-temperature (below 100°C) is a challenge with a great potential. Some specific applications are the following.

Low-concentration solar heat collectors Industrial-scale solar thermo-electric plants work at high temperature, with optical concentrators tracking the sun [8]. This technology is competitive with photovoltaics, but it can hardly be down-scaled to household application due to the need of bulky and cumbersome moveable mirrors. Rather, stationary non-imaging optics [9] coupled with vacuum tubes and selective adsorbers [10] could be used to collect heat at lower temperature. Such collectors are stationary and have an overall flat profile, similar to the ones normally used for domestic hot water production. Their efficiency is very high when working at a temperature of 100°C or lower, e.g., with a concentration factor of 2 and CERMET-based selective absorbers [11], 95% of sun power is collected.

Household co-generation Simultaneous room heating and production of electrical current by using fossil fuels is called “co-generation” or “combined heat and power”; the whole process has an increased efficiency with respect to the single processes. On industrial scale, a high-temperature heat engine exploits the heat of combustion and sends the low-temperature waste heat to the district heating network [12]. Household-scale plants have been studied [13]. Household applications would profit on devices able to handle heat released at low temperature. Condensing boilers are used to increase the fuel efficiency of heating, since they recover the latent heat of vaporisation of steam in the exhaust gases by condensation; in this case, co-generation would work at even lower temperature.

Low-temperature geothermal heat Classical geothermal power plants exploit high temperature geological heat sources. The global installed power is about 10 GW [14], mostly limited by the availability of the geological

sources. Geothermal sources below 100°C are widespread all over the world [15] but are currently not exploited mainly due to the lack of economically feasible technologies. Moreover, a geothermal gradient of approximately 25 K/km is available worldwide; it could be tapped by drilling relatively shallow wells.

Besides the small-scale applications, low-temperature heat is widely available as industrial waste heat. Various industrial processes consume energy for heating materials that must be then cooled down. It has been evaluated that 72% of the global primary energy consumption is lost after conversion [16]. As a rough estimate, up to 30% of the waste heat could be recovered [17]. In Europe, 23.7 TWh/year of electrical energy could be produced by recovery of waste heat [18]. A significant part of this heat is released at a temperature below 100°C. It has been argued that this heat could represent an alternative target of the low-temperature heat-to-current conversion techniques, although this idea is questionable, see ESI, Sect. S5.

The ability to exploit low-temperature heat sources, at small and household scale, to produce electrical current would have a more general consequence. In the field of electrical current, the importance of suitably networking different sources, storage devices, distribution power lines and final users has been emphasised (the so-called “smart grids”) [19], in particular at small and household scale. A concept of heat network also exists: thermoelectric and incineration plants are connected to district heating distribution networks; geothermal and solar heat are exploited for electrical power generation; seasonal heating and geological heat storage are used for household room heating. The electric and heat networks are already connected to each other by heat pumps. The possibility of connecting them in the reverse direction (convert heat into electrical current) locally, at small scale, would enable a fully integrated heat-current management system, aimed at optimising the available resources.

The traditional technologies that have been proposed so far for exploiting the low-temperature heat sources include heat engines [3] based on Stirling cycle [20] or organic Rankine cycle [21]. Although various attempts have been made to commercialise such devices, the cost is still too high (Capex 3-5 €/W) and they need too much maintenance (Opex 0.5 €/W/year) for enabling a widespread use. Moreover, the heavy maintenance that is needed makes them not suited for household applications, which are the most interesting for decreasing the environmental footprint of the energy production the various above-mentioned sources. Solid-state thermoelectric converters [22], based on Seebeck effect, have been tested: they require almost no maintenance but are even more expensive than the above-mentioned heat engines.

The challenge of developing innovative techniques has been taken on by the scientific community. In recent years, several papers were published on the subject. A large fraction is based on electrochemistry; some of the proposed techniques involve two stages, the first being a thermal treatment of a solution and the second the exploitation of such solutions for producing work, either mechanical or electrical. An authoritative review was recently published on such

techniques, giving an excellent overview of the various proposed methods [23]. At variance, the present review aims at presenting a critical comparison of the performances, with uniform metrics. The chosen performance indices are critical for the assessment of the technical and economical feasibility; indeed, some of the techniques fall below the feasibility limit by decades. We discuss the physical limitation of the performance indices for various techniques, when known, and the possible improvements. The scope includes the techniques able to handle heat sources at temperature less than 100°C; closely related techniques working at higher temperatures are also considered. The scope is similar to Ref. [23], with the addition of some more recent advancements. As in Ref. [23], thermal engines and solid-state thermoelectric converters are out of the scope; for literature on these topics, the reader is referred to the citations above.

Section 2 reports a short account of the working principles of the various reviewed techniques. We noticed that the various papers report the performances based on different criteria and working conditions; moreover, theoretical reasonings are often used to extrapolate the performances from experimental results. We introduce a uniform framework for the comparison of the results. The framework is described in Sect. 3, together with the comparison of the literature results. Care has been taken to ensure that the reported results are supported by experiments and are not only theoretical calculations. In some cases, we also report theoretical evaluations or hypothetical extrapolations from experimental results, but we mark them as such.

In various published works, it is suggested that an improvement of the performances can be obtained by combining several replicas of the same device, connected sequentially, in order to exploit multiple times the same amount of heat, at decreasing temperatures, or by using additional heat exchangers. This is what happens in some traditional technologies, such as in combined heat engines [24] and in multi-effect vacuum distillation [25]. The use of such techniques in the context of the exploitation of low-temperature heat sources is thoroughly discussed in Sect. 4.

Section 5 discusses the technological readiness level (TRL) and gives elements elements which are relevant for the evaluation of the technical and economical feasibility. The TRL is typically very low, so a complete evaluation is not feasible; rather we show that the performance indices enable a partial cost evaluation, which rules out some of the techniques (failing to reach the economical feasibility limit by decades) and identifies the most promising. For the latter, further theoretical and laboratory work is envisaged, in order to improve the performances, before their feasibility can be evaluated and judged competitive with the traditional techniques.

The results are discussed in Sect. 6. For some of the techniques, it has been shown that fundamental physical laws can be used to derive upper limits of the performances. Such limits can be used as a guideline for the comparison of the various techniques; in some cases, they are roughly approached by experimental realisations. Moreover, general thermodynamic methods have been used for interpreting the results of the experiments and for the design of improved techniques. An important example of such a general thermodynamic approach is

Short name	Description	Figure	References
TEC	Thermoelectrochemical cell, Thermogalvanic cell , electrochemical cell with two electrodes kept at different temperatures; equivalent to Seebeck effect.	1	See text
TREC	Thermally regenerative electrochemical cycle, Electrochemical heat engine , electrochemical cell that is charged at a temperature and discharged at a different temperature.	2	[26, 27, 28, 29, 30, 31] [32, 33, 34]*
CuACN	The Cu⁺ - ACN complex is destabilized by distilling off ACN, leading to disproportionation of Cu ⁺ into Cu and Cu ⁺⁺ , which, in turn, are used by an electrochemical cell to produce current.	3	[35, 36]
TRAB	Thermally regenerative ammonia battery , an electrochemical cell in which a voltage between two metallic electrodes is generated by the complexation of the cation in solution with ammonia or ammine, having different concentrations in the two compartments.	4	[37, 38, 39, 40, 41, 42, 43, 44]
TO	Thermo-osmosis , based on a porous membrane separating two liquids at different temperature. The vapour pressure difference generates a pressure between the two sides of the membranes. It drives a flux of liquid, which is sent to a turbine in order to generate work.	5	[45, 46, 47, 48, 49, 50, 51, 52]
TS-SGP	Thermal separation - salinity gradient power , the association of a device which generates two solutions at different concentrations, by exploiting heat, and a device which consumes the free energy of the solutions for producing work.	6	See Table 2

Table 1: List of the innovative techniques that are discussed in this paper. The first column reports the acronym, the second the definition and a short description, the third the number of the figure in this paper showing the scheme of the technique, and the last the bibliographic references. References marked with “*” refer to the supercapacitor-based TREC technique.

the analysis of the process in the temperature *versus* entropy graph, which is typical of the analysis of heat engines; it has been also applied to the techniques discussed in this review. When possible, the discussion of the techniques in Sect. 6 is based on such fundamental laws and general analysis methods.

2 Description of the techniques presented in literature

Table 1 reports the list of the techniques discussed in this review, together with the citations of the works discussing them. The focus is on techniques which are able to produce electrical or mechanical work by exploiting a heat source at $T_H < 100^\circ\text{C}$ and releasing the heat to a heat sink at room temperature T_L .

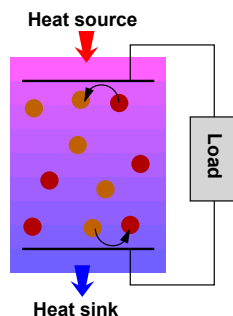


Figure 1: Sketch of a thermogalvanic cell. The two electrodes of an electrochemical cell are kept at different temperature. This condition generates a voltage across the electrodes, that is used to power a load.

Several of the schemes proposed up to now fall in the definition of “thermally rechargeable battery” (TRB). This is an electrochemical cell that produce electrical current, by consuming solutions that can be regenerated by a thermal process (either a chemical reaction or a thermal separation). The cell itself works isothermally, usually at room temperature. The reverse of this process is known as the “electrochemical cooling” [53]. Various TRBs, with good performances, have been described; unfortunately, many of them require a temperature much higher than the limit of 100°C [54] and are thus outside our scope. The techniques working at less than 100°C , falling in the definition of TRB, are the method based on Cu-acetonitrile complexation and Cu disproportionation (CuACN), the “thermally rechargeable ammonia battery” (TRAB), and a large number of variants of the thermal separation-salinity gradient power method (TS-SGP). The latter are so numerous that the references are reported in the separated Table 2.

Among the other reported techniques, there are the thermogalvanic cells, also called “thermo-electrochemical cells” (TEC), the “electrochemical heat engine” based on the so-called “Thermally regenerative electrochemical cycle” (TREC), and the thermo-osmosis (TO).

All these techniques are discussed in the following sections.

2.1 Thermogalvanic cells (TEC)

Thermogalvanic cells [55] or thermoelectrochemical cells (TECs) are an electrochemical equivalent of solid-state thermoelectric modules based on Seebeck effect. They are composed by a cell filled with an electrolyte, with two electrodes kept at different temperatures, as shown in Fig. 1. The two electrodes are usually made of the same electrocatalytic material. The electrochemical reaction taking place on the two electrodes is the same, however, thanks to the different temperature, a voltage arises between the electrodes. The voltage is

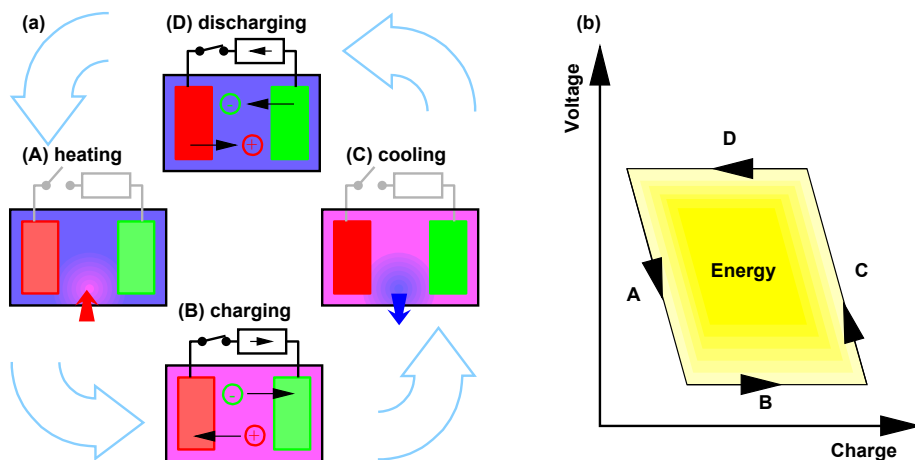


Figure 2: Sketch of the cycle of the electrochemical heat engine (a) and representation of the process in the voltage *versus* charge graph (b). An accumulator (either a battery or a supercapacitor) is sequentially heated (A), charged (B), cooled (C) and discharged (D).

roughly linear with the temperature difference between the two sides of the cell; the linearity coefficient α is an analogous of the Seebeck coefficient for thermogalvanic cells. In thermogalvanic cells, α is often 1-2 mV/K, competitive with typical solid-state thermoelectric elements.

This technique is relatively old and has been discussed in several reviews. We thus do not discuss it in detail and we refer the readers to the reviews cited above and to Refs. [56, 57].

2.2 Electrochemical heat engine (TREC)

The electrochemical heat engine is also called “thermally regenerative electrochemical cycle” (TREC). In this technique, an electrical accumulator (either a battery or a supercapacitor) is charged at a temperature and discharged at a different temperature. A review on this technique has been recently published [58].

The steps of the process, shown in Fig. 2a, are the following:

A heating The battery is heated to T_H using the heat source.

B charging The battery is electrically charged by an external source.

C cooling The battery is cooled down to T_L by releasing heat to the heat sink.

D discharging The battery is electrically discharged through the load.

As in TECs, the electrode potentials changes almost linearly with the temperature, with linearity coefficient α ; two electrodes, with different α , are chosen, so

that the temperature variation of the whole cell results in a variation of the cell voltage. Thus, due to the temperature variation, the voltage during discharging (D) is higher than during charging (B), while the charge flowing during charging and discharging steps is almost the same: this leads to a net power production. Figure 2b reports voltage versus charge graph; it can be noticed that the cycle is performed counter-clockwise, so that the area enclosed in the cycle represents the net delivered energy. It is worth noting that, in some of the reported TREC, the heating and cooling steps are reversed, i.e. the accumulator is charged after cooling: this depends on the sign of the value of α . This technique bears an analogy with the so-called “capacitive mixing” [59] and “battery mixing” [60], in which, at variance, the variation of voltage is induced by changing the salinity of the solution.

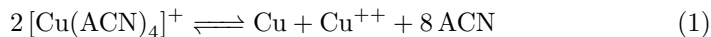
Several battery-like cells have been proposed, with various combinations of electrodes and electrolytes: i) copper *versus* copper hexacyanoferrate in $\text{Cu}(\text{NO}_3)_2$ solution [26]; ii) nickel hexacyanoferrate *versus* Ag/AgCl in KCl solution [27]; iii) Prussian blue $\text{KFe}_2(\text{CN})_6$ electrode in ferrocyanate solutions separated by a perm-selective membrane [28]. Schemes similar to a redox-flow battery have been studied, with $\text{Fe}(\text{CN})_6^{3-} / \text{Fe}(\text{CN})_6^{4-}$ as one of the redox couples, the other being $\text{Cu}(\text{NH}_3)_4^{2+} / \text{Cu}(\text{NH}_3)_2^+$ in Ref. [61] and $\text{V}^{++} / \text{V}^{+++}$ in Ref. [31]. In these devices, α is the order of a few mV/K.

In the case of supercapacitors, the electrodes are made of activated carbon [32, 34] or assemblies of activated carbons with polymeric membranes [33], dipped in salt solutions; the charge storage is obtained by the formation of electric double layers [62]. The variation of the voltage is due to the variation of the physical properties of the materials, in particular the relative dielectric constant of water. The temperature coefficient α is quite small, 0.6 and 0.3 mV/K in Refs [34] and [32], respectively. A hybrid method, with a capacitive and a battery-like electrode, has also been proposed [30].

Alternative schemes are partially related to TRECs: they are based on devices, other than batteries, able to accumulate energy. As TRECs, they are thermally cycled while charging and discharging. The proposed alternative devices are regenerative hydrogen fuel cells [63] or pressure-retarded osmosis devices [64]. Their performances have not been yet deeply studied up to now.

2.3 Method based on copper-acetonitrile complexation and disproportionation

Ref. [35] proposed a TRB in which the regeneration consists in distilling off acetonitrile from a water solution. The solution contains Cu^+ cations, stabilised by the formation of the complex $[\text{Cu}(\text{ACN})_4]^+$ (ACN=acetonitrile). During the distillation, the cation Cu^+ gradually undergoes disproportionation:



These physical processes have been exploited in the following cycle, schematically shown in Fig. 3:

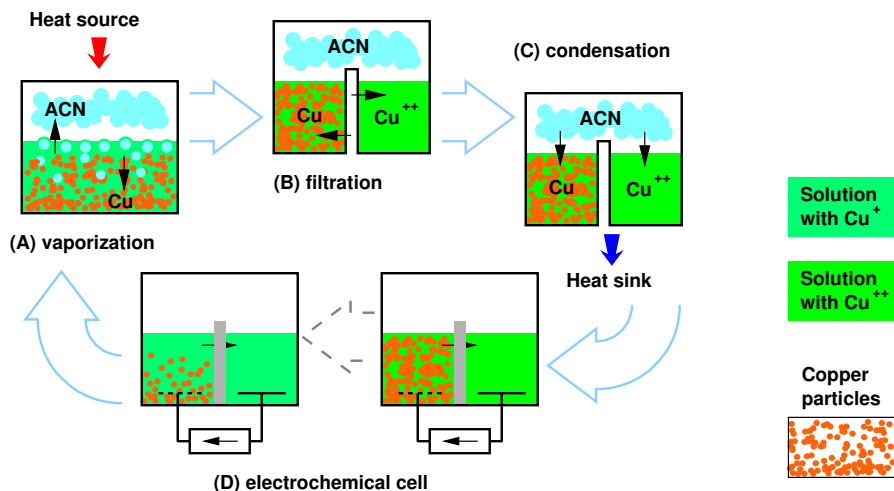


Figure 3: Sketch of the cycle of the method based on copper-acetonitrile complexation and disproportionation. The steps are: (A) heating, acetonitrile stripping and Cu^+ disproportionation; (B) separation of Cu particles by filtration; (C) condensation of acetonitrile by cooling; (D) exploitation of the solution and the slurry in the electrochemical cell.

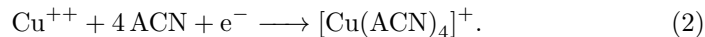
A vaporization Heat from the heat source is used to vaporize off acetonitrile from a solution containing $[\text{Cu}(\text{ACN})_4]^+$. Cu^+ disproportionates into metallic Cu particles and Cu^{++} in solution.

B separation The particles are separated by filtration, obtaining a dense slurry with Cu particles and a pure Cu^{++} solution.

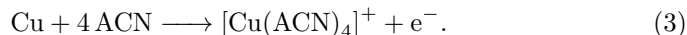
C condensation acetonitrile vapour is condensed by cooling and added back to the pure solution and to the dense slurry.

D electrochemical cell operation The electrochemical cell is fed with the Cu slurry and the Cu^{++} solution. It powers the electrical load and outputs the initial solution.

Mixing the liquids produced in step B, i.e. the slurry with Cu particles and the Cu^{++} solution, would eventually result in the irreversible comproportionation of Cu and Cu^{++} into the Cu^+ -ACN complex. By contrast, in the proposed process, the comproportionation is performed reversibly by the electrochemical cell, which thus extracts the available free energy. The electrochemical cell is composed by two compartments, separated by an anion-exchange membrane. The first compartment is fed with the Cu^{++} solution; the following reaction takes place on an inert electrode:



The second compartment is fed with the Cu particles, which are brought into contact with a current collector and constitute the electrode. They dissolve according to the reaction:



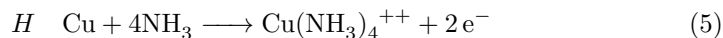
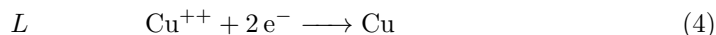
The cell converts (ideally all) the free energy of the solutions into electrical work. At the end of the electrochemical process, the solutions are ready to be regenerated, starting again the cycle from step (A).

In preliminary experiments [35] water solutions were used; the cell voltage was 0.62 V. Acetonitrile forms an azeotrope with water, and the distillation results in the removal of both water and acetonitrile. For this reason, in subsequent experiments [36], water was replaced by propylene carbonate, having a much higher boiling point. This increased both the efficiency of the regeneration step and the open-circuit cell voltage, which reached 1.3 V, the highest reported in this review.

Acetonitrile can be removed from the used acetonitrile - propylene carbonate mixture at around 80°C at 1 atm; however, in the presence of Cu⁺, distilling off part of acetonitrile requires a higher temperature, around 160°C: this temperature is required for destabilising the complex.

2.4 Method based on ammonia complexation

The first proposed “thermally regenerative ammonia battery” (TRAB) [37] was based on complexation of Cu⁺⁺ ions by ammonia. The cycle is schematically shown in Fig. 4. The electrochemical cell is composed by two compartments, *L* and *H*, separated by a perm-selective membrane, filled with solutions containing Cu⁺⁺ ions, with copper electrodes. The compartment *H* also contain ammonia, which complexes Cu⁺⁺ ions. The electrochemical equilibria of the two compartments are reached at different potentials. The resulting cell voltage of 0.44 V generates a current that is used to power a load, through the following reactions in the two compartments *L* and *H*:



According to the reactions, the copper electrode in *H* dissolves, the one in *L* is plated and the Cu⁺⁺ concentrations change accordingly. As Cu⁺⁺ is depleted in *L*, the cell voltage decreases, until the discharge is stopped. Then the solution in *H* is sent to a distillation column, driven by the heat source at around 70°C, for stripping ammonia and sending it to the opposite compartment, so that the cycle can start again.

During the full cycle, the role of the compartments *L* and *H* are cyclically exchanged. Focusing on one of the compartments of the cell, the steps of the cycle are the following, starting with a high concentration of ammonia in the compartment:

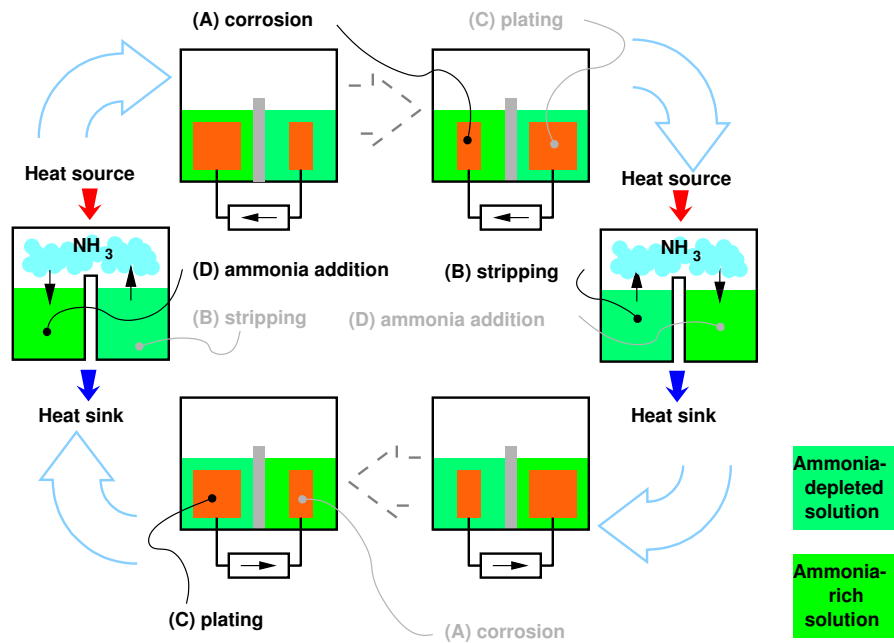


Figure 4: Sketch of the method based on complexation of Cu^{++} by ammonia. The two compartments of the cell contain a solution with Cu^{++} ions; one also contains ammonia. Focusing on one of the compartments, the cycle steps are (A) corrosion, (B) ammonia stripping, (C) plating, and (D) ammonia addition (black labels). The opposite compartment makes the cycle (C), (D), (A), and (B) (grey labels).

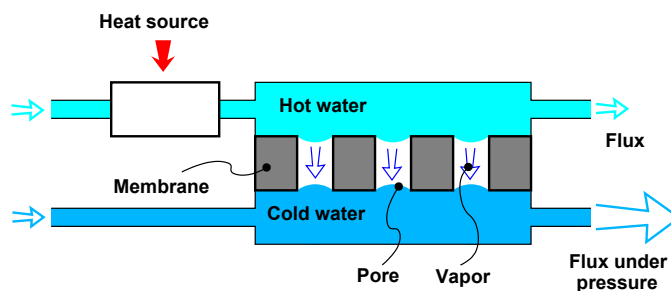


Figure 5: Sketch of the thermo-osmosis method. Water at different temperatures is put into contact with the two sides of the membrane. This condition generates a water flux across the membrane, also resulting in the development of a pressure, which represents a mechanical work.

A corrosion A current flows through the cell and the load, so that the copper electrode is corroded, releasing $\text{Cu}(\text{NH}_3)_4^{++}$ ions.

B stripping The solution in the compartment is treated in the distillation column in order to remove ammonia, which is sent to the opposite compartment.

C plating A current flows through the cell in the opposite direction; copper is plated on electrode.

D ammonia addition Ammonia stripped from the solution in the opposite compartment is added to the solution.

From the point of view of the other (opposite) compartment, the sequence of steps would be (C), (D), (A), and (B).

The same concept was further developed with practical realizations [38, 39] and numerical calculations [40]. Alternative chemistries were also studied. Among them, Ag^+ ions and complexation with ammonia [42] and Cu^{++} ions complexed with ethylenediamine [41]; in the second case, the cell voltage increased to 0.6 V. The use of two different metals in the two compartments, Cu and Zn, has also been suggested [43, 44]. In this case, a non-vanishing cell voltage is always present; by means of ammonia complexation and ammonia stripping, the cell voltage is changed between cell discharge and charge, so that the two operations are performed at different voltages, 0.98 V and 0.76 V for discharge and charge, respectively. A net energy is gained, corresponding to a voltage rise of 0.22 V, much less than in the other cases reported above.

2.5 Thermo-osmosis

This method is also called “pressure-retarded membrane distillation” [45, 46]. A porous, hydrophobic membrane separates two fluxes of pure water. One of

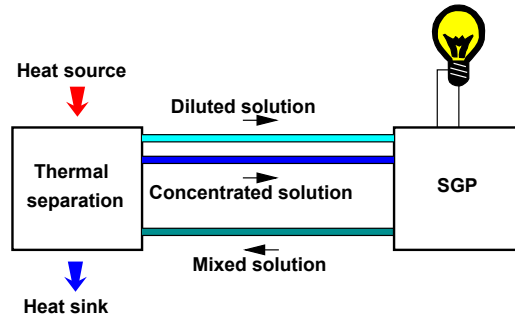


Figure 6: Sketch of the thermal separation - salinity gradient power technique. A solution is separated into concentrated and diluted solutions by exploiting a low-temperature heat source. The solutions feed a salinity gradient power device. The consumed (mixed) solution is sent back to the thermal separation to close the cycle. Various techniques can be used to implement the thermal separation and the salinity gradient power units; they are listed in Table 2 and described in detail in Sect. 2.6.

the fluxes is put into contact with the heat source, so it enters in the membrane module at a higher temperature than the other. Thanks to the different temperature, the vapour pressures of the fluids at the two sides of the membrane are different, so that water tends to evaporate from the hot liquid and condense in the cold liquid. This flux can withstand an opposite pressure of the order of 10 bar, thus it makes work that can be tapped by means of a turbine. The whole device also requires a pressure exchangers, as usual in PRO [65].

Theoretical [47] and experimental [50] works showed that the limit of the pressure is due the membrane deformation which takes place at high pressure, which is detrimental for the vapour flux. This phenomenon practically limits the pressure to around 10 bar. Performances of highly technological carbon nanotube membranes have also been discusses [49, 51].

Thermo-osmosis can also be exploited in membrane distillation desalination plants, possibly powered by low-temperature heat sources, in order to produce electrical energy together with desalinated water. Theoretical analysis [52] and experimental investigations of the physical principles [48] of the coupled processes have been carried on.

2.6 Thermal separation - salinity gradient power

The general concept behind the thermal separation - salinity gradient power technique (TS-SGP) is sketched in Fig. 6. The process is cyclical and the steps are the following:

A thermal separation A solution is separated into concentrated and diluted solutions by exploiting a low-temperature heat source.

	PRO	RED	BattMix	Redox-flow	Generic
Vacuum dist. (VD)	[66]	[67, 68, 69, 70, 71, 72]	[73, 74]	[75, 76]	[77, 78, 79]
Membr. dist. (MD)	[80, 81, 82]	[83, 84]			
Thermolysis (TL)	[85]	[86, 87, 88, 89, 90, 91, 92, 93] [94, 95]*	[96]		
Other	[97]		[98]		
Generic	[99]	[100, 101]	[60]		

Table 2: List of the techniques based on thermal separation - salinity gradient power closed cycle. Each cell contains the bibliographic references for the combination of SGP (columns) and TS (rows) techniques. The references marked with “*” refer to microbial RED cells. The columns and rows labelled “Generic” refer to papers that only focus either on the thermal separation or on the salinity gradient power technique.

B salinity gradient power The solutions at different concentration feed the SGP device, i.e. a device that produces work by consuming a concentration difference, thus producing work.

The output of the SGP device, step (B), is constituted by the mixed solutions; it is sent back to the thermal regeneration stage, step (A). In literature, this scheme is sometimes referred to as “closed loop SGP”.

A remarkable advantage of the TS-SGP technique is its intrinsic ability to store energy, in the form of solutions at different concentrations. The energy is temporarily stored in the form of mixing free energy of the solutions, while other TRBs exploit different forms of chemical free energy [54].

Several different thermal separation processes have been proposed in literature. They are shortly accounted in the following list. The literature references are reported in Table 2.

Vacuum distillation (VD) The heat is used for distilling off the solvent from a solution. The device is composed by two chambers: in the “boiler”, the heat from the heat source is used to vaporise the solvent of the solution; the vapour is then condensed in the “condenser” [102]. In order to boil solvents at low temperature (e.g. water below 100°C), air is evacuated from the whole system, so that it operates under vacuum. It is worth noting that rigorously no additional mechanical work is needed for keeping the vacuum, because the system is a closed loop and no air is admitted, while a small mechanical work is usually needed for open systems.

Membrane distillation (MD) Several methods fall under this definition [103]. The feed solution and the distilled solvent are kept separated by a hy-

drophobic porous membrane, which ensures the separation of the liquids while allowing the passage of the vapour. The heat exchange surface is large, so it is possible to operate the system at a pressure above the boiling point of the solution, exploiting the solvent evaporation rather than boiling it. Such systems are typically more compact than vacuum distillation.

Thermolysis (TL) When a solution of ammonium carbonate is heated, the salt dissociates and is evolved from the solution in the form of ammonia and carbon dioxide gases; this phenomenon is called “thermolysis”. In TS-SGP, a distillation column is used [104]. The spent solution coming from the SGP device is sent to the column inlet. A dilute salt solution is extracted from the reboiler, while a concentrated salt solution is produced by the condenser.

Other methods It has been proposed to use ionic liquids which undergo a phase separation below a critical temperature [97], so that they separate into two solutions at different concentrations by cooling. A patent [98] covers a process in which the concentration difference is generated by the crystallisation of a solute induced by temperature decrease.

Various technologies have been developed for producing electrical work by exploiting concentration differences, i.e. for SGP; the production of current takes place at the expense of the mixing free energy of the solutions, which become eventually mixed. The study of the SGP technology has initially aimed at tapping the mixing free energy of naturally occurring solutions, such as sea water versus river water [105], as a clean source of energy. With this aim, several techniques have been developed, among them: pressure-retarded osmosis [106] (PRO), reverse electrodialysis [107], capacitive mixing (CapMix) [59] and battery mixing [60].

Some of such techniques have been applied to the context of TS-SGP, operating in closed loop with one of the TS methods discussed above; moreover, specific techniques have been developed on purpose. The following list reports a short description of them. The literature references are reported in Table 2.

Pressure-retarded osmosis (PRO) The two solutions flow on the two sides of a semipermeable membrane, i.e. a membrane which allows the passage of the solvent but not of the solute. An osmotic flux of solvent develops across the membrane, which is able to flow against a quite large hydraulic pressure. The liquid flux represents a mechanical work done by the solutions [106]. Usually, it is assumed that the liquid flux is fed to a turbine in order to generate electrical current.

Reverse electrodialysis (RED) Two solutions, containing different concentrations of ions, flow on the two sides of a perm-selective membrane. The membrane allows the diffusion of charges with a given sign, which constitutes an electrical current [107]. Anionic and cationic membranes are usually assembled to form a stack.

Capacitive and Battery mixing (CapMix and BattMix) An electrochemical cell is sequentially filled with the two solutions with different concentrations. The cell is electrically charged and discharged at different concentration of solution. Due to the concentration variation, the cell is charged at a voltage less than the voltage present during the discharge, thus giving a net energy production at the expense of the mixing free energy of the solutions [59].

Concentration redox-flow batteries (CRFB) These devices bear analogies with the redox-flow batteries [108]. The overall effect of the discharge is that the concentration difference between the two compartments of the cell decreases, at variance with the traditional redox-flow batteries, in which the overall effect is the variation of the oxidation state of the electrolytes. The design includes an unconventional device that performs a liquid-liquid exchange; moreover, the electrochemical cell makes use of solid-state permselective membranes, which enables operation at very high concentrations.

Various combinations of TS and SGP techniques have been studied; the literature references are reported in Table 2.

3 Comparison of the performances

In this section we discuss the performances of the techniques comparing them on a uniform basis. The framework for the comparison is chosen based on the target applications, i.e. small-scale exploitation of low-temperature heat sources, with $T_H < 100^\circ\text{C}$.

3.1 Efficiency

The energy efficiency η is the ratio between the produced work (either electrical or mechanical), W , and the heat from the heat source, Q_H :

$$\eta = \frac{W}{Q_H}. \quad (6)$$

Working with a heat source at temperature T_H and a heat sink at T_L (typically, room temperature), the energy efficiency is limited by the Carnot law, $\eta < \eta_C$, where η_C is the efficiency of the Carnot cycle:

$$\eta_C = \frac{T_H - T_L}{T_H}. \quad (7)$$

In the reviewed papers, the efficiency $\eta_{2nd-law}$, defined as follows, is also used:

$$\eta_{2nd-law} = \frac{\eta}{\eta_C}. \quad (8)$$

It is the ratio between the actual energy efficiency and its maximum η_C , according to the second law of thermodynamics, hence the name “2nd-law efficiency”.

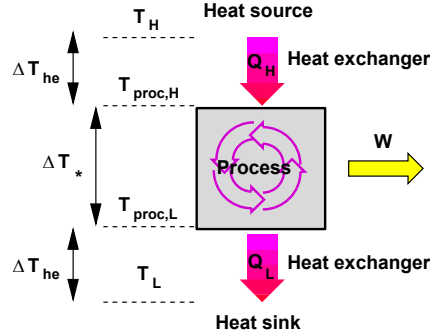


Figure 7: The processes discussed in this review require two heat exchangers, one from the heat source and one to the heat sink.

The scope of this paper includes thermal machines having a heat input from the heat source, a heat output to the heat sink (environment), and a work output. For such machines, $\eta_{2nd-law}$ actually corresponds to the exergy efficiency.

The efficiency is one of the performance indices that we use in this review, since it is relevant for the target applications stated above. It must be noticed that, in some applications outside the scope of this review, the efficiency is not a particularly relevant parameter: it is for example the case of the energy scavenging for powering wireless electronic devices, of energy harvesting for Internet-of-things, or of wearable devices [109].

We decided to compare the energy efficiency η , rather than $\eta_{2nd-law}$. The detailed discussion choice, with examples, is reported in ESI, Sect. S1. Summarising, the heat collection device must be seen as a capital cost, while the revenues are represented by the produced work. The low-temperature heat is never completely “for free”, due to the cost of the heat collection system. When evaluating the various techniques, it is thus interesting to know how much work is produced by a given heat collection system, which is well represented by η . Instead, having a large $\eta_{2nd-law}$, operating on a small temperature range, thus corresponding to a small η , is not necessarily economic.

The idea that the low-temperature heat sources are not “for free” is also clarified in Fig. 7, which shows that at least two heat exchangers are always present in the techniques reviewed here: one connecting the process to the heat source and one to the heat sink. Due to these heat exchangers, the upper and lower temperature seen by the process, $T_{proc,H}$ and $T_{proc,L}$, respectively, are different from T_H and T_L by ΔT_{he} , the temperature drop across the heat exchanger. The temperature difference available to the process, $\Delta T_* = T_{proc,H} - T_{proc,L}$, is thus smaller than $T_H - T_L$, giving a smaller Carnot limit efficiency. In the application to low temperatures, it is thus critical to keep ΔT_{he} small, which means that large and expensive heat exchangers are needed per unit of heat transferred from the heat source.

3.2 Assumptions on the performances of additional heat exchangers

Various methods have been proposed to increase the efficiency by means of “multi-effect” combination of devices or “heat recuperation”; we call them collectively “multi-effect combination and heat recuperation schemes” (MEHRS). They are thoroughly discussed in Sect. 4. The term “heat recuperation” must not be confused with the “heat recovery”, which is instead the name often given to the general idea of exploiting waste heat. The MEHRSs are based on the use of additional heat exchangers with respect to the two shown in Fig. 7 (see Figs. 9 and 10); they significantly increase the complexity, the size and the cost of the plant. In principle, such schemes are actually able to improve the efficiency of the various techniques, however, the improvement depends on the performances of the heat exchangers. In the reviewed works, no MEHRS has been studied experimentally; instead, hypothesis on the possible performances of the heat exchangers are made. In several cases, the reported efficiency of the technique is calculated based on the assumption of “infinite-sized heat exchangers”, see e.g. Ref. [46]: “*Our analysis reveals that an optimized system can achieve heat-to-electricity energy conversion efficiencies up to 4.1% [...]. Lower energy efficiencies, however, will occur [...] with finite-sized heat exchangers.*” This approach is quite naïve, as any technique has to deal with finite-sized heat exchangers: even a Carnot cycle does not approach the Carnot efficiency unless infinite-sized heat exchangers are “used”. It is often found that the different performances reported in papers on similar techniques depend mostly on the different assumptions on the heat exchangers, rather than on real improvements of the technology.

In order to give a fair comparison, in this section the performances of the techniques that use MEHRS are reported on a uniform basis assuming a temperature difference across heat exchangers ΔT_{he} of 5 K; extrapolations are made when the information found in papers is insufficient. The chosen value, $\Delta T_{he}=5$ K, is larger than the value used in most of the papers, however, it is still so small that it is hardly feasible in practical plants. Since the MEHRS are often considered in literature, in Sect. 4 we thoroughly discuss them and the effect they have as a function of ΔT_{he} . Here, we anticipate the result: the MEHRS mostly improve the performances of the least performing techniques but does not make them competitive with the most performing one; changing ΔT_{he} does not change the overall ranking of the techniques given here (i.e. with $\Delta T_{he}=5$ K), unless impractically small values of ΔT_{he} are assumed.

3.3 Power density

The second performance index that we analyse is the power density p . The geometry of the devices suggests to express it as power per unit surface. In order to give a fair comparison of the various techniques, care has been taken to use a uniform definition of the involved surface. Most of the discussed techniques are based on membranes, which often represent a significant cost of the

system; in such cases, the surface used in the calculation is the surface of the membranes [40]; care is taken to convert the values that are given *per membrane couple*. In the other cases, we consider the section of the cell. Moreover, in the case of batch processes, we decided to report the average power density rather than the peak power density.

3.4 Comparison of literature results

For each technique, we calculated the energy efficiency η and the power density p from the data reported in the references cited in Tables 1 and 2. Only a few works are completely experimental; in the majority, at least one part of the system is simulated numerically. In the analysis reported here, we only report results that are at least mostly experimental. Works partially making use of numerical calculations are also taken into consideration, only if the part of the process evaluated theoretically belongs to a well assessed field, having a high TRL. In some cases, different parts of the process are discussed in different papers; we pay attention to evaluate the overall performances relative to compatible working conditions. Some results are reported as open symbols; they represent overestimations, coming from partially theoretical calculations or from evaluation of η and p in different conditions.

The detailed discussion of all the papers, based on the above-described framework, is reported in ESI, Sect. S2. The results are summarised in Fig. 8. Each point corresponds to a result reported in a paper; the correspondence between points and literature reference numbers are shown in ESI, Fig. S1.

4 Multi-effect combination and heat recuperation schemes

Many of the reviewed papers propose the use of a MEHRS, i.e. scheme involving additional heat exchangers in order to improve the performances of the technique. In order to be effective, the temperature drop across the heat exchangers, ΔT_{he} , must be small. While the decrease of ΔT_{he} increases the efficiency, it is obtained by increasing the surface of heat exchangers, which is expensive, as noticed in Ref. [68]: “*the amount of heat exchanger area [...] [represents] an important share of the total capital costs of the unit.*”. For this reason, it is necessary to add a performance index to the techniques which use a MEHRS, namely the power production per unit surface of heat exchangers.

4.1 Multi-effect combination and heat recuperation schemes (MEHRS)

Figure 9 schematically shows the combination of processes in series, as in the “multi-effect distillation”. Two heat exchangers connect the heat source and sink to the system and further heat exchangers connect multiple processes in

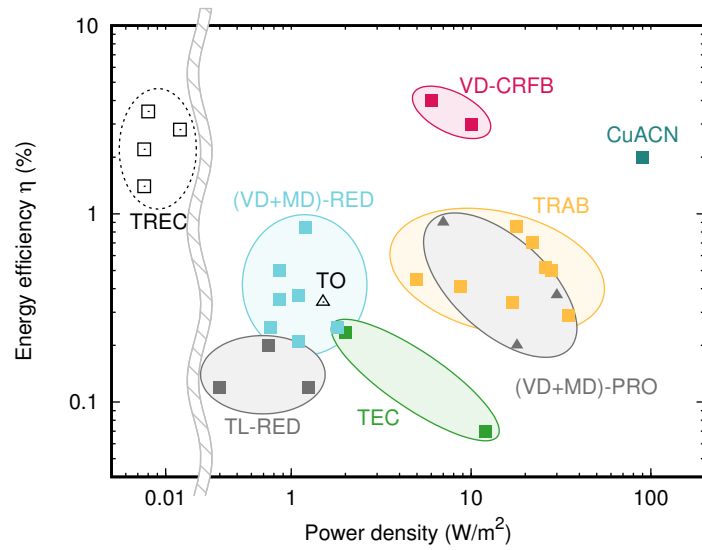


Figure 8: Comparison of literature results. When MEHRS (multi-effect or heat recuperation) are used, the performances are reported for $\Delta T_{he}=5$ K (extrapolations are done when necessary). The horizontal axis is broken in order to show the power density of TRECs. Open symbols and dotted lines represent either theoretical limits or overestimations. Squares refer to electrochemical methods, triangles refer to mechanical methods (requiring a turbine).

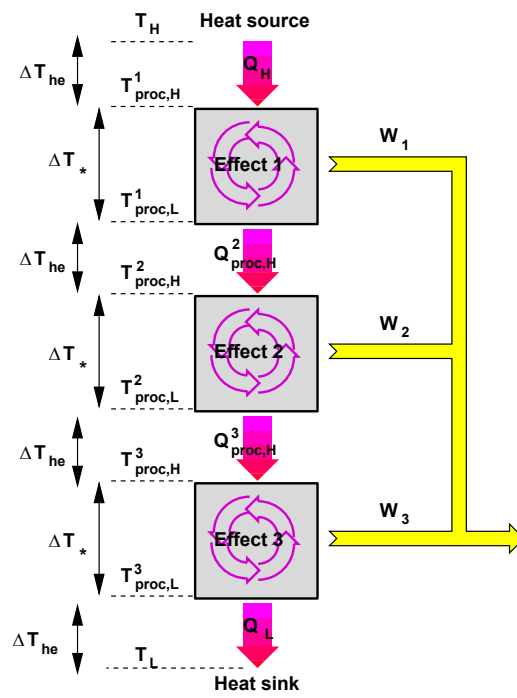


Figure 9: Scheme of the combination of multiple processes in series. The consecutive processes work at decreasing temperatures, and the heat that exits from an effect feeds the following.

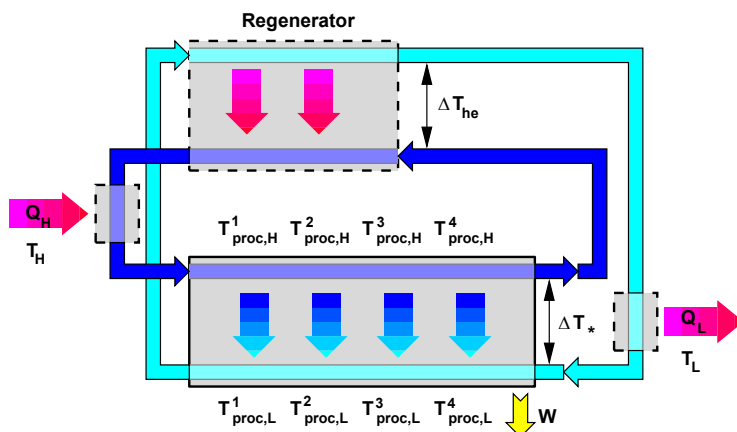


Figure 10: Scheme of the “heat recuperation”. The heat source and sink are in thermal contact with the fluids in two circuits. The exchange of heat between the fluids takes place in counter-current, on the bottom side through the processes, and on the top side through the counter-current heat exchanger.

sequence, so that the heat released by a process is sent to the following. Combining in series various processes is aimed at exploiting the available heat more than one time. It has been proposed for the distillation-based techniques (VD-PRO, VD-RED, VD-BattMix and VD-CRFB) and for thermolysis-based techniques [87]. The aim is to utilise the same heat in a sequence of processes, each taking place across a temperature difference ΔT_* that is smaller than the available temperature difference $T_H - T_L$. It must be noticed that Fig. 9 is a generalisation of the concept: when multi-effect vacuum distillation is used, the output of each effect is not directly a work W , but rather the mixing free energy of the produced solutions.

A different scheme has been proposed for membrane distillation, called “heat recovery” [110]. It is shown in Fig. 10. It is based on two hydraulic circuits in which two fluids fluxes in counter-current. In the top part of the scheme, we see a heat exchanger between the two fluids; on the bottom, there is still a counter-current heat exchange, but it takes place through the processes (segments of the membrane distiller). The heat source and sink at T_H and T_L are thermally connected to the two fluxes. Thanks to the counter-current heat exchange, part of the heat can be recovered and utilised again by the processes. This scheme has been proposed for the techniques based on membrane distillation (MD-PRO and MD-RED) and for TO. Also in this case, the figure is a generalisation of the concept, e.g. it does not show the SGP device connected to the membrane distillation module.

A third scheme, also called “heat recuperation”, has been used for TREC. In this technique, the heat source provides the reaction heat during the electrical

discharge, but it must also provide the sensible heat for bringing the temperature of the cell to T_H . In the proposed MEHRS, part of this heat is provided by the sensible heat of another cell, which is undergoing the cooling step of the process. Although this scheme bears similarities with the “heat recuperation” of Fig. 10, in this case the heat involved in the MEHRS is only a fraction of the heat provided by the source (the sensible heat and not the reaction heat).

4.2 Power density per heat exchanger surface

The performance index introduced in this section is the power per unit surface of heat exchangers:

$$\rho = \frac{P}{S} \quad (9)$$

where P is the produced (electrical or mechanical) power and S is the surface of heat exchangers.

This performance index is connected to the energy efficiency and to the temperature drop across the heat exchangers, ΔT_{he} . In order to generate a work W , an amount $Q_H = W/\eta$ of heat is needed from the heat source, but a larger amount Q_{he} will cross the heat exchangers. As an example, in the case of a n effects (see Fig. 9), almost the same amount of heat Q_H crosses all the effects, thus $Q_{he} \approx Q_H n$. In order to keep the temperature difference across the heat exchangers as low as ΔT_{he} , the needed surface S is:

$$S = \frac{\dot{Q}_{he}}{\Delta T_{he} \cdot U} \quad (10)$$

where U is the heat transfer coefficient, a parameter that depends on the heat exchanger nature and technology. The power density per heat exchanger surface, ρ , is thus:

$$\rho = \frac{P \cdot \Delta T_{he} \cdot U}{\dot{Q}_{he}} \quad (11)$$

The value of U is typically assumed to be 1000 W/(m² K), for both vacuum distillers [69] and for heat exchangers between solutions [110]. In a few papers, slightly different values of U are used. The heat exchanger technology is not discussed in detail, nor experiments with practical realisations of heat exchangers are reported, thus the different values are not significant and should be not attributed to differences in the performances of the discussed techniques.

In order to provide a uniform evaluation of ρ , independent on the performances that are assumed in the various papers, we decide to evaluate ρ with the uniform value $U_0=1000$ W/(m² K) for all the techniques. In the few papers in which slightly different values of U are used, we recalculate ρ based on $U_0=1000$ W/(m²K). Calculated in this way, the performance index ρ is genuinely connected to the heat-exploiting technique, independently on the its possible implementations with different heat exchanger techniques. If a specific heat exchanger technique is utilised, with a given U , the actual power per unit surface of heat exchangers can be calculated as $\rho U/U_0$.

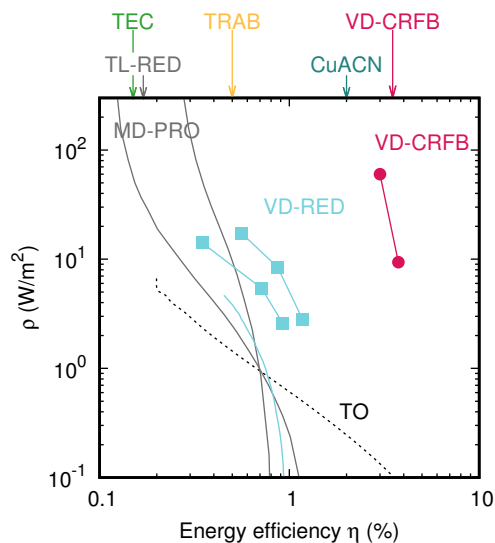


Figure 11: Dependence of ρ on the energy efficiency η for various techniques which make use of MEHRS. The efficiency of the techniques which do not make use of a MEHRS is reported above the graph; the vertical position is not related to any value of ρ .

Heat exchangers between the heat source and the process and between the process and the heat sink are needed by all the discussed techniques (see Fig. 7). For this reason, these two heat exchangers are not taken into consideration in the calculation of ρ and do not participate to the MEHRS heat exchanger surface S .

4.3 Trade-off between ρ and η

Some of the reviewed papers report η and ρ for various values of ΔT_{he} . The resulting ρ versus η curves are shown in Fig. 11. The techniques which do not make use of a MEHRS are reported above the graph; for them, only the horizontal position, η is relevant. The detailed discussion of each paper is reported in ESI, Sect. S3

In Fig. 11, it can be clearly noticed that there is a trade-off between η and ρ : the efficiency η can be increased at the expense of a larger amount of heat exchangers per unit produced power. For example, the TO device discussed in Ref. [45] can in principle reach an efficiency of more than 4%, larger than the efficiency of the VD-CRFB system discussed in Ref. [75], but the required heat exchangers are almost three decades larger. The trade-off between η and ρ has been already noticed and discussed in literature, e.g. the graph in Fig. 6f of

Ref. [68] shows that the efficiency increases together with the heat exchanger area, as the temperature difference across the heat exchangers decreases.

It has been shown that the shape of the ρ versus η curves, such as the ones reported in Fig. 11, can be easily calculated based on the applied MEHRS [111]. An approximated calculation is straightforward for the multi-effect combination. The energy efficiency η is:

$$\eta = \eta_* \cdot n \quad (12)$$

where n is the number of effects and η_* is the energy efficiency of a single effect. In order to calculate ρ from Eq. 9, we first notice that the heat flowing through each heat exchanger is almost the same, \dot{Q}_H (approximating $\dot{Q}_L = \dot{Q}_H(1 - \eta) \approx \dot{Q}_H$, all effects are crossed by \dot{Q}_H , see Fig. 9), thus:

$$\dot{Q}_{he} = (n - 1) \cdot \dot{Q}_H = (n - 1) \frac{P}{\eta}; \quad (13)$$

here we remind that the heat flux considered in \dot{Q}_{he} excludes the heat exchangers with the heat source and the heat sink, hence the considered heat exchangers are $n - 1$ (see Fig. 9). Using Eq. 9 we get:

$$\rho = \eta \frac{U \cdot \Delta T_{he}}{n - 1} \quad (14)$$

In turn, n can be approximately evaluated by dividing the available temperature range by the temperature drop across each effect:

$$n = \frac{T_H - T_L - \Delta T_1}{\Delta T_{he} + \Delta T_*} \quad (15)$$

where ΔT_1 is the temperature drop across the heat exchanger from the heat source. Here, we assume that ΔT_* is equal for all the processes and ΔT_{he} is uniform across the heat exchangers and equal for all the heat exchangers. When the multi-effect system is a multi-effect vacuum distiller, ΔT_* is actually the boiling point elevation of the solution. Calculating:

$$\eta = \eta_* \frac{T_H - T_L - \Delta T_1}{\Delta T_{he} + \Delta T_*} \quad (16)$$

$$\rho = \eta_* U \Delta T_{he} \frac{T_H - T_L - \Delta T_1}{T_H - T_L - \Delta T_1 - \Delta T_{he} - \Delta T_*} \quad (17)$$

These two last expressions give η and ρ parametrically in ΔT_{he} , for a given temperature range defined by T_H and T_L , once the technique has been characterised by η_* and ΔT_* . This means that, even after making use of a MEHRS, the relative performances of the techniques are dependent on the performances of the single stages, i.e. a technique with a more efficient single stage will outperform a less efficient technique when a MEHRS is applied to both.

An analogous procedure has been applied to the ‘‘heat recuperation’’ MEHRS [111]. Quite surprisingly, the result is that the performance indices η and ρ are formally equal to the expressions for the multi-effect, Eqs. 12 and 14. Ref. [111] reports

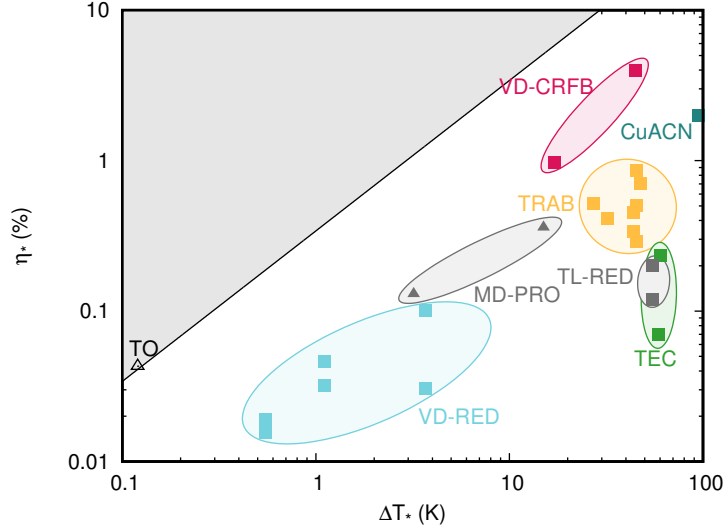


Figure 12: Comparison of the techniques in the η_* versus ΔT_* graph. Open symbols represent theoretically evaluated maximal values rather than experimental results. The diagonal line represents the Carnot limit.

small differences between the two schemes, which are however not relevant for the analysis carried out here.

The validity of the approximated Eqs. 16 and 17 is discussed in ESI, Sect. S4, by showing that they fit the results of several papers. These approximations have been discussed in the context of vacuum distillation [78, 79].

4.4 Intrinsic performance indices ΔT_* and η_* .

It can be noticed that Eqs. 16 and 17 give η and ρ as a function of T_H , T_L , ΔT_{he} , ΔT_* , and η_* . Only the last two, ΔT_* and η_* , are characteristic parameters of the technique: they represent the temperature difference across a single effect and its energy efficiency, respectively; by contrast, T_H , T_L , ΔT_{he} are parameters describing the MEHRS. This suggests us to use ΔT_* and η_* as intrinsic parameters of the technique, net of the possible improvements that can be obtained by using a MEHRS.

Fig. 12 shows the placing of the various techniques in the η_* versus ΔT_* graph. The calculation of each value from the corresponding paper is reported in ESI, Sect. S4. The identification of each point appearing in Fig. 12 is reported in ESI, Fig. S6. It can be noticed that the various techniques operate on a large range of ΔT_* covering almost three decades. The best techniques have an efficiency 3-10 times smaller than the Carnot cycle.

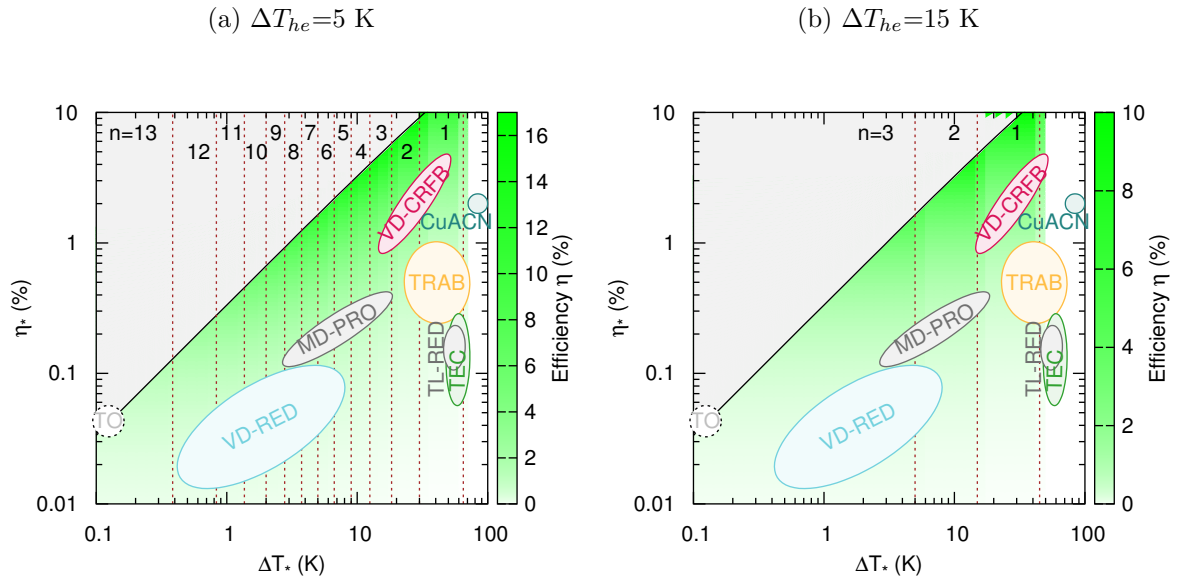


Figure 13: Energy efficiency η obtained using a multi-effect MEHRS, represented in false colours as a function of η_* and ΔT_* . $T_H=100^\circ\text{C}$ and $T_H=25^\circ\text{C}$. The black diagonal line represents the Carnot limit. The ellipses represent the distribution of performances of the various techniques; dashed ellipses represent theoretical maximum performances rather than experimentally measured values. The numbers on the top part of the graph are the number of effects, separated by vertical dashed lines. Two values of ΔT_{he} are reported.

Following Ref. [111], based on the values of η_* versus ΔT_* , it is possible to theoretically calculate η and ρ attained by using a MEHRS, with a given ΔT_{he} , operating on a temperature range from T_L to T_H . Results are shown in Fig. 13, in false colours superposed on the η_* versus ΔT_* graph, where the various techniques are also represented.

In Fig. 13, the energy efficiency is calculated for multi-effect MEHRS [111], for two values of ΔT_{he} . The number of effects is shown on the top of the area of the graph; $n = 1$ actually means that no MEHRS is used.

For techniques for which $\Delta T_* \ll \Delta T_{he}$, decreasing ΔT_* allows us to increase the number of effects, but this does not increase the efficiency η at same η_* which is obtained with the MEHRS. In order to reach a large efficiency η , it is thus not useful to have a large $2nd$ -law efficiency at low ΔT_* , but rather a high efficiency η_* , which, in turn, requires a large ΔT_* . The best efficiencies η are obtained by techniques with large η_* ; techniques with small ΔT_* , and thus small η_* , get the largest advantages from the MEHRS, but do not become competitive with techniques with larger η_* , in particular for $\Delta T_* < \Delta T_{he}$.

The necessity for a large η_* is even more evident when the heat exchanger surface is taken into account. The techniques with ΔT_* around 10 K and a large $2nd$ -law efficiency have an efficiency η up to 4%, with a single effect (i.e. no MEHRS is actually applied). By contrast, techniques with ΔT_* of the order of 1 K require 10 or more effects in order to reach an efficiency lower than 1%: this increases the complexity of the system and requires large surfaces of heat exchangers.

The discussion does not qualitatively change in the case of the “heat recuperation” scheme [111]. This analysis shows that η_* plays the role of performance index relevant for both the energy efficiency η and the heat exchanger power density ρ of the techniques using a MEHRS. The techniques which reach the highest η_* are MD-CRFB and CuACN, which do not require any MEHRS and which were already recognised as the most promising techniques in Fig. 8.

Summarising, the techniques with a high η_* yield the best performances, also with MEHRS; techniques with a small η_* profit on the MERHS, but do not become competitive with techniques with high η_* . This result can be surprising, since it is different from what happens with high-temperature heat sources, and is specific to the case of low-temperature heat sources, where $T_H - T_L$ is comparable with ΔT_{he} .

4.5 Approximate expressions for η and ρ

Following Ref. [111], the concepts discussed in the previous sections can be expressed alternatively by performing an approximation of Eqs. 16 and 17. The approximation of η and ρ is obtained for $\Delta T_{he} + \Delta T_* \ll T_H - T_L$, i.e. for a large number of effect n :

$$\eta = \eta_* \frac{T_H - T_L}{\Delta T_{he} + \Delta T_*} \quad (18)$$

$$\rho = \eta_* U \Delta T_{he} \quad (19)$$

Here we notice that η_* directly fixes ρ , once ΔT_{he} has been chosen: this remarks once again the importance of η_* .

It is useful to calculate $\eta_{2nd-law}$ from Eq. 16:

$$\eta_{2nd-law} = \eta_* \frac{T_H}{\Delta T_{he} + \Delta T_*} \quad (20)$$

where we approximated $\Delta T_1 = 0$. Defining the $2nd$ -law efficiency of a single process:

$$\eta_{2nd-law,*} = \eta_* \frac{\Delta T_*}{T_{proc,H}}, \quad (21)$$

we can further approximate this expression as:

$$\eta_{2nd-law} = \eta_{2nd-law,*} \frac{\Delta T_*}{\Delta T_{he} + \Delta T_*} \quad (22)$$

This equation can be used as a rule of thumb for selecting ΔT_{he} : given a process with $2nd$ -law efficiency $\eta_{2nd-law,*}$, the overall $2nd$ -law efficiency of the MEHRS will be close to $\eta_{2nd-law,*}$ if $\Delta T_{he} \ll \Delta T_*$, but will vanish for $\Delta T_{he} \gg \Delta T_*$.

5 Technical and economical feasibility

5.1 Technology readiness level

The TRL of all the technologies discussed in this paper is very low. The techniques reported in Table 1 are between TRL 2 and 3, i.e. the fundamental principles have been observed and the technology concept has been formulated, however, a complete realization of the whole process has not been performed yet, not even at laboratory scale. Thanks to the relatively smaller experimental complexity, TECs are the most close to the laboratory validation of the whole device. On the opposite side, the evaluation of TO has mostly been performed theoretically. Details of the specific techniques are given in Sect. 6.

The same TRL range is reached by TS-SGP techniques, listed in Table 2: usually, only one of the two parts, TS or SGP, is tested in the experiments and the overall performances of the TS-SGP combination are only theoretically calculated. The only exception is Ref. [88], in which a TL-RED device is presents; unfortunately, the performances are not satisfactory and worse than expected and shown in Fig. 8.

Since TS-SGP is composed by the combination of two technologies, it is useful to first give a separate evaluation of the TS and the SGP stages. Distillation (VD and MD) are at fully commercial stage. TL has been tested in small laboratory scale, but the underlying technology (column distillation) is also at fully commercial stage. The other separation technologies are at TRL 2. None of the SGP techniques is at commercial stage, however, pilot plants based on PRO and RED have been built for exploitation of naturally occurring salinity gradients. CapMix and CRFB are at TRL 3.

This notwithstanding, it must be noticed that the association of TS and SGP require more scientific effort than simply combining the techniques: as explained in previous sections, the design requires to develop the understanding of the underlying thermodynamics of the system. An example is VD-RED, where distillers with 20 or more effects (seldom used in practice) have been studied. For this reason, we evaluated a TRL between 2 and 3 for the TS-SGP techniques. Details of the specific techniques are given in Sect. 6.

Due to the low TRL, a complete and reliable technical and economical assessment is not yet feasible. Rather, we aim at showing how the selected performance indices are critical for determining the technical and economical feasibility: they enable at least a partial technical and economical analysis, which allows us to rule out some of the techniques and to direct the research towards the most promising.

5.2 Partial evaluation of costs based on p and η

The heat exploited by the various techniques cannot be considered as available “for free”. At least, heat exchangers are needed to collect the heat, and heat exchangers contribute to the cost of the whole device. Since the power output of the system is proportional to η , the cost per unit installed power contains a term which is inversely proportional to η . The heat collection cost depends on the collection technique; as an example, in ESI, Sect. S6, we discuss the case of solar heat collection by means of stationary, household-scale collectors. The evaluated cost per installed unit heat power is $c_h=0.2 \text{ €/W}$. This quantity must be divided by η to give the contribution of heat collection to the overall cost, c_h/η .

We expressed the power density p as the power per unit surface, because all the discussed techniques are based on thin foil-like elements, either membranes or relatively thin electrodes, characterised by a surface. Such elements have a cost per unit surface c_s . The discussion of c_s is reported in ESI, Sect. S7: the cost is optimistically evaluated in the range $c_s=50\text{-}150 \text{ €/m}^2$, depending on the technique, although much more expensive elements could be needed. This quantity must be divided by p to give the contribution related to surface area to the overall cost, c_s/p .

It must be emphasized once again that the two mentioned costs, i.e. c_h/η , the cost of heat collection and c_s/p , the cost related to surface area, are only a part of the whole cost. This evaluation is not aimed at an overall evaluation of the feasibility of the techniques, but it can rather prove that some of them are very far from feasibility, simply considering one of the various aspects, i.e. based on p or η alone. This shows that the chosen performance parameters are critical for the evaluation of the economic feasibility.

By using the costs c_h and c_s reported above, the heat collection cost is of the order of $c_h/\eta=5 \text{ €/W}$ at the highest η , i.e. 4%, and the cost related to surface area is of the order of $c_s/p=1 \text{ €/W}$ at the highest p , i.e. 100 W/m^2 . As a comparison, photovoltaic cells have a cost per unit peak power less than 0.5 €/W , likely with a longer duration than electrodes and membranes, and a

whole household-scale installed plant costs less than 2 €/W. The various reported techniques span decades in p and η below the best performance indices; it can be clearly seen that some of them are definitely not economically feasible, although further research will likely improve the performances. The analysis shows the relevance of the performance indices p and η for a preliminary screening of the techniques, useful also in the absence of a complete technical and economical feasibility analysis. It is worth noticing that the costs per installed heat power collection, c_h , and the cost proportional to the surface area, c_s , are within a relatively small range, while the values of η and p span decades. The values of p and η reported in the previous sections, together with the discussion about the possible improvements and physical limitations given in the followings section, can be used to rule out some of the techniques and focus on the most promising ones. Moreover, this discussion highlights that the performance indices p and η are currently the most critical for the feasibility of the techniques.

5.3 Cost of heat exchangers

We introduced the performance index ρ , describing the power per unit surface of heat exchangers, in order to characterise the performances of a MEHRS. Its relevance is emphasised by observing that heat exchangers have a cost per unit surface, c_{he} , which significantly contributes to the total cost of the device [68].

In Ref. [112], the cost of heat exchangers used in VD is in the range $c_{he}=200-400$ €/m². This high cost is in agreement with the claim found in Ref. [68] that the amount of heat exchanger area represents an important share of the total capital costs of the VD-RED units. In the following, we use this value range, although it can be different for different types of heat exchangers [113].

The contribution of the heat exchangers used in MEHRS on the total cost per unit installed power is c_{he}/ρ ; it vanishes for techniques which do not use MEHRS. The values of ρ are shown in Fig. 11 for various techniques. As an example, a value of $\rho=1$ W/m² corresponds to a very high cost of 200-400 €/W.

A further insight can be gained by considering the partial cost $c_{he}/\rho + c_h/\eta$, i.e. the sum of the cost of heat collection and of heat exchangers in the MEHRS. As ΔT_{he} decreases, η increases but ρ decreases: the partial cost can be thus optimised by suitably choosing ΔT_{he} . The optimal value of ΔT_{he} can be theoretically evaluated using the expressions of η and ρ as a function of the intrinsic performance indices η_* and ΔT_* , expressed by Eqs. 16 and 17. We already showed that such expressions are accurate. The resulting partial cost $c_{he}/\rho + c_h/\eta$ is thus expressed as a function of ΔT_{he} and can be minimized [111].

Here we report the results obtained with the simplified Eqs. 18 and 19. We first use the simplified equations to express the partial cost $c_{he}/\rho + c_h/\eta$, then we calculate value of ΔT_{he} which minimises it. The result is:

$$\Delta T_{he} = \sqrt{\frac{c_{he}}{c_h} \frac{T_H - T_L}{U}} \quad (23)$$

Using again Eq. 19:

$$\frac{c_{he}}{\rho} = \frac{c_{he,*}}{\eta_*} \quad (24)$$

where:

$$c_{he,*} = \sqrt{\frac{c_{he}c_h}{U(T_H - T_L)}} \quad (25)$$

The term $c_{he,*}$, with the assumptions and approximations discussed above, is of the order of 1 €/W. Although this value can change, depending on the specific technique, this result highlights the importance of the performance index η_* : while the partial cost c_h/η can be reduced by using a MEHRS, the cost c_{he}/η_* only depends on the intrinsic performance index η_* , which cannot be increased by the MEHRS. The values of η_* , reported in Fig. 12, say that the partial cost c_{he}/η_* is of the order of 1 €/W for the best performing techniques, while it goes to more than 1000 €/W for the lowest η_* . This analysis confirms that the MEHRS do not change the ranking of the techniques, i.e. techniques with large η_* are needed and, for such techniques, MEHRS are not needed, and highlights that the performance index ρ is one of the most critical for the feasibility of the techniques.

5.4 Occupation of space and complexity of the system

The size of a device working with a given technique is an important parameter, particularly when dealing with devices that are meant for household application. The performance index p can be quite directly related to a volume, although this volume is only a part of the whole system. As remarked above, all the discussed techniques are based on thin foil-like elements, either membranes or relatively thin electrodes. The performance index p represents the ratio between the produced power and the surface of such elements. On the other hand, the thickness of a single cell composed by such elements is of the order of magnitude of 1 mm, although the geometry of the devices depend on the specific technique. In some of the techniques, TEC and some TREC, the electrolyte does not flow between the electrodes; this enables the use of thin spacers, of the order of 100 μ , which adds up to the electrode thickness and to the current collectors, giving a total cell thickness not much smaller than 1 mm. In all the other cases, a liquid flow is needed, thus the minimum cell thickness is limited by the necessity of keeping the hydraulic resistance low.

If we assume that this thickness is 1 mm, as a rough approximation for all the techniques, we see that the cells of a device able to produce a peak power of 5 kW with $p=10$ W/m² has a volume of 500 L; it must be emphasised once again that this is only a part of the total volume. Although bulky, such a volume could fit into a room of a private house. However, it must be noticed that the values of p span decades, so it is apparent that some of the techniques require a too large volume, just considering the cells; some of them also require cumbersome additional parts, e.g. the techniques based on PRO require a turbine.

A similar reasoning can be applied to ρ ; in this case, the characteristic thickness to be evaluated concerns the heat exchangers. This thickness is limited by

the necessity of keeping the hydraulic resistance small. If the thickness is below 1 mm, the device is considered a “micro heat exchanger”, while much larger sizes are typically seen in industrial applications. We thus see that the situation is similar to the case of the performance index p : with $\rho=10$ W/m² the heat exchangers occupy 500 L, under the optimistic assumption of thickness of 1 mm. This additional volume could be much larger, since, in some of the techniques, a suitable efficiency (in turn connected with the cost of heat collection, as discussed above) is only obtained with very small ρ , as shown in Fig. 11.

It is worth noting that a small value of ρ does not only affect the size of the system but also its complexity. For example, in the case of VD, a small value of ρ is connected with a large number of effects (up to 20 or more in some evaluations) and a small temperature difference across the heat exchangers, ΔT_{he} (even below 1 K in some evaluations). Both requirements are technically hard to fulfil and significantly contribute to the complexity of the system.

6 Discussion of the techniques based on fundamental physical principles

The various reviewed techniques cover a wide range in the $\eta - p$ and $\eta_* - \Delta T_*$ graphs, Figs. 8 and 12, respectively. As clarified in the previous sections, the most performing techniques are in the top-left corner of both graphs. In this section we discuss the performances of the various techniques, aiming at explaining the placing in the $\eta - p$ and $\eta_* - \Delta T_*$ graphs based on fundamental physical principles.

6.1 Thermogalvanic cells (TEC)

The performances of the cell are mostly determined by three parameters: the thermoelectric coefficient α (see Sect. 2 for the definition), the heat conductivity and the heat cell resistance (in turn, depending on electrolyte resistivity and electrode properties). Roughly, α and resistance determine the power at a given temperature difference. The cell voltage is of the order of tens of mV, and the power density is small, compared to other electrochemical devices such as batteries.

The TECs are inherently in non-equilibrium: the two sides of the cell are kept at different temperatures. The energy efficiency is the ratio between the produced power and the heat flux, mostly due to heat conduction. Heat convection can be decreased by using gels or porous matrices [109], however, the conduction cannot be eliminated and is an intrinsic property of the chosen materials. Although no physical limitation to the efficiency has been evidenced in literature, besides the Carnot limit, from the results reported in literature, it appears that the efficiency of TECs is actually much less than the Carnot efficiency; this is eventually due to the properties of the currently used materials. Quoting Ref. [58]: *As a result, the typical efficiency is limited to an equivalent*

ZT of <0.1 (e.g., efficiency is 0.7% of Carnot efficiency (η_C) at $\Delta T=5$ K). This translates into $\eta=0.01\%$.

Efficiency η depends on the properties of the materials; it is typically very small, the best results being of the order of 0.1%.

Temperatures ΔT_* can be adapted to any available temperature difference. However T_H is limited by parasitic reactions.

MEHRS No MEHRS is required.

Power p is usually very low, due to the small cell voltage. Optimised systems reach power densities of the order of 1 W/m². Power densities up to 10 W/m² have been obtained at the expense of an even smaller efficiency than other TECs.

Level of development Thanks to the relatively simple design, the laboratory-scale devices are relatively similar to real-world realisations.

Overall remarks The technique has the remarkable advantage of being simple and compact. It is probably well suited for very-small-scale energy scavenging, in which high efficiency is not as important as compactness.

6.2 Electrochemical heat engine (TREC)

As in the case of TECs, the power is defined by the overall thermoelectric coefficient α (difference between the thermoelectric coefficients of the two electrodes) and the cell resistance. In the experiments reported in the reviewed papers, the power is even smaller than in TECs.

At variance with TECs, no direct heat conduction takes place; rather, heat is parasitically transported from the heat source to the heat sink by the sensible heat of the cell. The process can be ideally carried on close to reversibility. It has been argued that this different mechanism of heat transfer would increase the energy efficiency with respect to TECs.

A sketch of the temperature T versus entropy S graph is shown in Fig. 14. The charging (B) and discharging (D) phases are isothermal; in order to follow the cycle clockwise (produce energy), the chemistry of the battery is chosen so that the charging (B) and discharging (D) phases are exothermic and endothermic respectively. The slope of the heating (A) and cooling (C) steps is due to the heat capacity of the battery.

We notice that the cycle in the T versus S graph covers a diagonal band, rather than approaching the Carnot cycle (cyan rectangle), due to the exchange of sensible heat in steps (A) and (C). In the reviewed papers, the sensible heat exchange Q_A and the reaction heat Q_B are calculated based on an ideal cell composition, and they appear to be of the same order of magnitude, e.g. in Ref. [26] they are $Q_A=60$ J/g and $Q_B=45$ J/g per unit mass of active material (see ESI). In the experimental realisations reported in the reviewed papers, Q_A is however much bigger than Q_B , thus the area covered by the cycle, represented

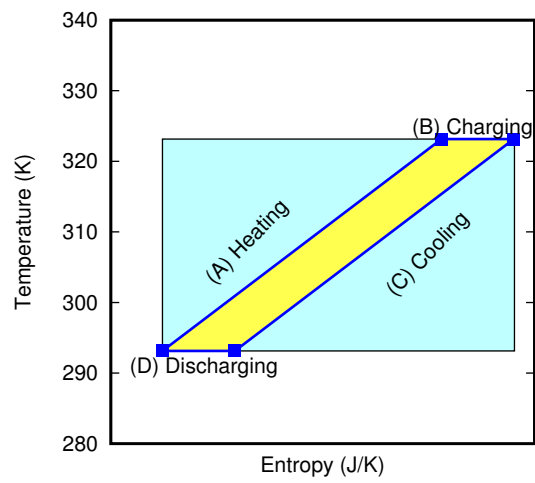


Figure 14: Sketch of the temperature *versus* entropy diagram of the cycle of the electrochemical heat engine. An accumulator (either a battery or a supercapacitor) is sequentially heated (A), charged (B), cooled (C) and discharged (D). The yellow area represents the produced electrical work, while the cyan area is the Carnot cycle. The temperature approximately correspond to the experiment presented in Ref. [26] while the entropy scale is arbitrary.

in yellow in Fig. 14, is a diagonal band, covering much less than the Carnot cycle (cyan rectangle).

It must be emphasised that the reported efficiencies refer to theoretical calculations, in which Q_A only takes into consideration only the sensible heat of the active materials; no real cell, approaching that value, has been demonstrated and the passive elements of the cell have not been discussed.

Heat recuperation of the sensible heat could improve the situation, however, it would be based on solid-solid heat exchange (heat exchange between cells), thus its feasibility is questionable in practice.

The works on TREC report the power production per unit mass of active material, which translates into a very small power per surface, of the order of 10 mW/m^2 , due to small electrode mass loading (a few mg per cm^2). It has been argued that a larger power could be hypothetically achieved with larger mass loading of active materials (see e.g. Ref. [23], reporting larger power density). However, the extrapolation to larger mass loading is questionable and has never been tested in experimental cells. Based on literature on batteries, increasing the mass loading is detrimental for the performances, in particular it increases the overvoltages; TRECs are even more sensitive than batteries to this effect, because they work with a voltage rise much smaller than cell voltage of typical batteries.

It is worth noting that some of the experiments [34, 26, 27] were performed with a heat sink temperature T_L lower than room temperature, namely 0°C , 10°C , and 15°C , in Refs. [34], [26, 31], and [27], respectively. This low temperature heat sink is not always naturally available. In the case of battery-like cells [26, 27], the use of the low temperature was necessary in order to have a large temperature difference $T_H - T_L$ while keeping T_H low enough to avoid parasitic reactions (see e.g. Fig. 4 of supplementary information of Ref. [26]). The choice of refrigeration in the case of supercapacitors [34] is likely due to a similar reason, i.e. to avoid charge leakage.

Efficiency η is limited by the ratio between the reaction heat (steps (B) and (D)) and the exchanged sensible heat (steps (A) and (C)). Only theoretical maximum values have been discussed in literature.

Temperatures In principle ΔT_* can be adapted to any available temperature difference. However T_H is limited by parasitic reactions to less than $60\text{--}70^\circ\text{C}$.

MEHRS No MEHRS is required.

Power p is very low, of the order of 10 mW/m^2 , due to the small cell voltage and small active material loading. It could be probably increased by optimising the working conditions but experiments are missing up to now.

Level of development The physical principles have been demonstrated. Most of the performance evaluations are theoretical.

Overall remarks The technique has the theoretical potential exploit the whole temperature range from the heat source at $T_H=60-70^\circ\text{C}$ down to room temperature. The theoretical maximum value of η is interesting, however, it has not been demonstrated in practical operation; it is questionable if this theoretical limit can be practically approached. In the experimental works, the power density p is impractically small. The technique still requires laboratory experimental work.

6.3 Method based on copper - acetonitrile complexation (CuACN)

Experiments on this technique were performed using a temperature $T_H=160^\circ\text{C}$, i.e. above the temperature that is in the scope of this review, $T_H=100^\circ\text{C}$. This is partially the reason of the high energy efficiency η with respect to the other techniques.

Since two different processes are involved, namely the thermal and the electrochemical processes, it is worth separating the efficiency η into the product $\eta_{TP} \cdot \eta_{EP}$ of the thermal process efficiency η_{TP} and the electrochemical process η_{EP} . The former is defined as the ratio between the free energy ΔG of the produced solution and the consumed heat Q_H :

$$\eta_{TP} = \frac{\Delta G}{Q_H} \quad (26)$$

while the latter is defined as the ratio between the produced electrical work W and the available free energy ΔG :

$$\eta_{EP} = \frac{W}{\Delta G} \quad (27)$$

The most limiting term is η_{TP} . Its value can be usefully discussed based on the temperature *versus* entropy graph [114] shown in Fig. 15. The area highlighted in yellow represents the free energy of the solutions that are fed into the electrochemical cell (see the discussion of the temperature *versus* entropy graph in Ref. [77], which also applies to this case; rigorously, the operation of the electrochemical cell should be excluded from the calculation). The graph can thus be used to graphically discuss the efficiency of the thermal process, η_{TP} , which is the ratio between the area highlighted in yellow and the area of the Carnot cycle, the cyan rectangle.

The heat consumption takes place at two different plateaus, marked as “vaporisation” and “reaction”, which correspond to the vaporization of acetonitrile and to the dissociation of the Cu-ACN complex, respectively. It can be roughly assumed that the area below the “vaporisation” segment corresponds to the increase of mixing free energy of the solutions, while the area below the “reaction” is the free energy associated with the complexation. Both are available to the electrochemical cell.

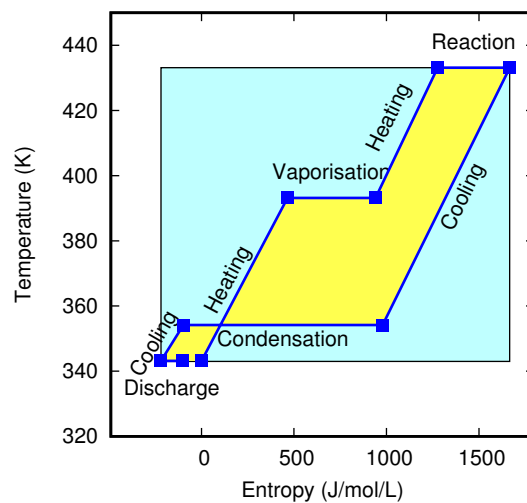


Figure 15: Example of temperature *versus* entropy of the CuACN process [114], with 1.5 M Cu^{++} solution and 30% acetonitrile in propylene carbonate. The yellow area represents the produced electrical work, while the cyan area is the Carnot cycle.

From the temperature *versus* entropy graph, it can be clearly seen that the cycle covers a relevant part of the ideally rectangular Carnot cycle. The significant advantage of this technique is that the cycle covers a high temperature difference of around 80 K; this intrinsically give a large Carnot efficiency, and does not require the use of MEHRS.

Efficiency η is one of the largest reported in the reviewed papers, approximately 2%.

Temperatures ΔT_* is around 90 K, the largest reported in this review. A single stage can thus cover the available temperature range between T_H and T_L . No MEHRS is required. It must be noticed that $T_H=160^\circ\text{C}$, higher than the maximum temperature of heat sources considered in the other reviewed papers.

MEHRS No MEHRS is required.

Power p is very high, around 100 W/m^2 , thanks to the high cell voltage.

Level of development The whole process has been realised in laboratory. The single parts of the process have not been integrated into a automatic process.

Overall remarks The technique has a very good potential and the experimental demonstration is sound. The main challenge for increasing the TRL will likely be the handling of the copper nanoparticle slurry.

6.4 Thermally regenerative ammonia battery (TRAB)

These techniques show a relatively small energy efficiency below 1% with a quite high power density.

The process has been studied thoroughly, however, no clear explanation for the observed performances has been given, nor fundamental principles have been shown to limit them. More in general, the energy efficiency of column distillation, defined as ratio between produced free energy of solutions and consumed heat, has not been widely studied; Ref. [115] tackles the problem but is not focused on energy production from heat sources, nor considers the presence of complexes in the solutions.

Efficiency The values of η fall in the centre of the range of η of the various techniques, slightly below 1%. The reviewed papers do not report ideas to improve it.

Temperatures ΔT_* is quite large, from $T_H=70\text{-}80^\circ\text{C}$ to room temperature.

MEHRS No MEHRS is required.

Power p is interesting, of the order of 10 W/m^2 .

Level of development The whole process has been realized in laboratory. The single parts of the process have not been integrated into a automatic process.

Overall remarks The technique has a quite high power density but the efficiency is small, compared with other techniques. It is not clear if and how the efficiency can be improved, in order to enable practical applications.

6.5 TO

Ref. [45] discusses the theoretical maximum of the energy efficiency. Given a temperature difference ΔT_* across the membrane, the maximum generated hydraulic pressure is calculated based on Antoine and Kelvin equations. The heat flux from the heat source is calculated taking into account only the latent heat of evaporation. From such assumptions, the maximum energy efficiency is found to be the Carnot efficiency.

It is worth noting that this calculation neglects the large contribution of the membrane heat conduction, which is usually relevant [110, 81].

It has been noticed that the vapour flux strongly decreases at hydraulic pressures of more than 10 bar [45, 47, 50]. Since ΔT_* is a function of the pressure, this pressure limitation represents a limit to the temperature difference across the membrane, $\Delta T_* < 0.12$ K. In turn, this limits the efficiency of the process (without MEHRS) to $\eta_* < 0.043\%$. These values of ΔT_* and η_* allow us to calculate the energy efficiency η with the MEHRS, following the discussion reported in Sect. 4; the results are consistent with the performances reported in Ref. [45] when the MEHRS is applied (see ESI, Sect. S3). We thus see that this pressure limit is the reason for the poor placing of this technique in Fig. 12: it limits ΔT_* , which in turn limits η_* . In turn, η_* limits η to very small values, hence the poor placing of TO in Figs. 8.

The pressure limit has been attributed to a mechanical deformation of the membrane [47, 50], however, experimental confirmations of the deformation have not been provided.

The power production has been experimentally evaluated and reaches the order of magnitude of 1 W/m^2 . However, the experiments proving such a power production were conducted in conditions under which the efficiency was predicted to be even smaller than reported above.

Efficiency η_* is limited by the maximum pressure, $\eta_* < 0.043\%$. This strongly limits the practical applicability of the technique with real (finite-sized) heat exchangers. Real efficiencies are even smaller, due to heat conduction across the membrane, which have not been characterised.

Temperatures ΔT_* is limited to 0.12 K by the pressure limitation.

MEHRS High efficiencies are only feasible with extremely large surfaces of heat exchangers, even theoretically. For example, producing 1 kW with an efficiency $\eta=1\%$ would require a heat exchanger of around 1000 m^2 , assuming ideal conditions.

Power p of the order of 1 W/m^2 has been evaluated experimentally, but under working conditions under which η vanishes (i.e. η_* is even much smaller than 0.043%). Experiments are still needed to evaluate the power production under non-vanishing efficiency.

Level of development The physical principles have been observed. Most of the evaluations are based on theoretical extrapolations.

Overall remarks Increasing 10-100 times the pressure limit of the membranes would be necessary to make this technique competitive with the others.

6.6 Distillation-salinity gradient power (TS-SGP)

In this technique, two different processes are involved, namely TS and SGP. It is thus worth separating the efficiency η into the product $\eta_{TS} \cdot \eta_{SGP}$ of the TS efficiency η_{TS} and the SGP efficiency η_{SGP} . The former is defined as the ratio between the mixing free energy ΔG of the produced solution and the consumed heat Q_H :

$$\eta_{TS} = \frac{\Delta G}{Q_H} \quad (28)$$

while the latter is defined as the ratio between the produced electrical work W and the available mixing free energy ΔG :

$$\eta_{SGP} = \frac{W}{\Delta G} \quad (29)$$

The same separation can be done for η_* , which can be written as the product $\eta_{TS,*} \cdot \eta_{SGP}$, where $\eta_{TS,*}$ is the energy efficiency of a single TS stage of a MEHRS.

The efficiency $\eta_{TS,*}$ is usefully discussed based on the temperature *versus* entropy graph. It is easy to show [77] that the area covered by the cycle (yellow area in Fig. 16) represents the produced mixing free energy; thus the ratio between the area covered by the cycle (yellow area) and the area of the Carnot cycle (cyan area) represents the 2nd-law efficiency $\eta_{2nd-law}$.

6.6.1 Vacuum distillation (VD)

The temperature *versus* entropy graph for vacuum distillation is shown in Fig. 16. The process consists in the following steps:

A Heating The mixed solution is heated up to the boiling point

B Boiling Part of the solvent is vaporised

C Cooling The solution and the vapour are cooled down

D Condensing The vapour is condensed

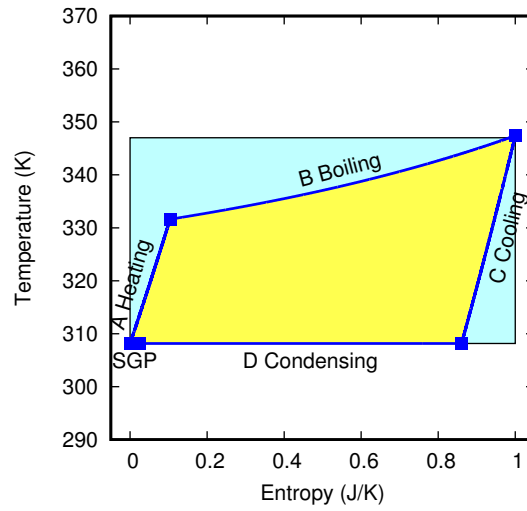


Figure 16: Distillation process represented in the temperature *versus* entropy graph. The distilled solution is NaOH in water, having a high boiling point elevation. The yellow area represents the produced electrical work, while the cyan area is the Carnot cycle. The data are taken from Ref. [79].

The temperature difference between steps (B) boiling and (D) condensing is the boiling point elevation of the solution, corresponding to ΔT_* ; in the example of Fig. 16, it is high because of the use of an extremely concentrated solution of NaOH; ΔT_* of a few K are typical of more dilute solutions often used with RED. The increase of temperature during step (B) boiling is due to the increase of concentration of solution during solvent vaporisation, which leads to the increase of boiling point elevation. The slope of steps (A) heating and (C) cooling are due to the sensible heat provided or captured from the solution.

The efficiency of vacuum distillation has been discussed in Refs. [78] and [79]. Some of the results can be easily interpreted by discussing the temperature *versus* entropy graph: i) the area enclosed by the cycle increases with increasing boiling point elevation, which is the height of the cycle ΔT_* ; ii) In order to increase the efficiency $\eta_{TS,*}$, the segments (A) heating and (C) cooling should be as much vertical as possible, compared to the width of the cycle; this corresponds to decreasing the heat capacity of the solutions with respect to the latent heat of vaporisation; iii) the slope of the segment (B) boiling should be as horizontal as possible. From these points, we conclude that the used solutions must have a high boiling point elevation, a large latent heat of vaporisation and a small heat capacity [78, 79].

The first two design rules (high boiling point elevation and large latent heat of vaporisation) could appear as counter-intuitive for researchers working in the field of distillation, since they are detrimental for the produced volume of distillate and concentrate. However, in the context of TS-SGP, the aim is to produce the largest amount of mixing free energy rather than the largest volume of distillate or concentrate, hence the different design rules. On the other hand, the requirements are not surprising in the field of heat engines, e.g. in Rankine cycle, it is well known that a large latent heat of vaporisation has a positive effect.

The increase of efficiency $\eta_{TS,*}$, and in turn of η_{TS} , with increasing boiling point elevation has been highlighted in several papers, e.g. Refs. [77, 78, 79, 67, 69] and has been experimentally observed in others. For example, in Ref. [82], higher efficiency is obtained with methanol solutions than with aqueous solutions of LiCl, likely because of the higher ebullioscopic constant. Fig. 11a of Ref. [67] shows the increase of efficiency with increasing concentration; in the case of multi-effect distillation (panel b of the same figure), the data are reported for $\Delta T_{he}=2$ K, a very small value, but the effect would be much more visible taking a larger and more realistic ΔT_{he} . Other papers identify highly soluble salts as more promising [69], since they provide a higher boiling point elevation.

The discussion above refers to $\eta_{TS,*}$ and η_{TS} ; now we discuss the SGP techniques that have been coupled with vacuum distillation. In the case of RED, η_{SGP} drops at high concentration [116], due to loss of perm-selectivity occurring when the membrane charge density becomes comparable with the ionic strength of the solution; a dramatic increase of resistivity also occurs at high concentration, due to the osmotic removal of solvent from the membrane. For VD-RED techniques, there are thus competing requirements: η_{TS} increases with increasing boiling point elevation, and thus with increasing concentration,

but η_{SGP} decreases with increasing concentration. This concentration limitation also leads to a limited power density, of the order of a few W/m^2 . A similar limitation is found for PRO, in which concentration polarisation pose a limit to the concentration; according to the results of Figs. 8 and 12, the advantage of PRO seems to be a larger power density p compared with RED.

This situation has been emphasized in several papers, where the improvement of performances is eventually connected to the development of future “high-performing membranes” [68], “high performing IEMs” [69], or “ideal IEMs” [70], able to work at higher concentration. For example, Ref. [69] clearly identifies this problem as the bottleneck of VD-RED technique, showing that the limitation comes from the poor ability of current RED membranes to handle high concentrations.

An alternative approach has been proposed based on CRFBs [75, 76]. The innovative design of such redox-flow batteries includes an unconventional liquid-liquid extraction device and a solid-state ion-conducting membrane, which easily withstands concentrated solutions and overcomes the above-discussed bottleneck. The result is impressive, as it can be seen in Figs. 8 and 12: the VD-CRFB technique outperforms all the VD, MD, and TL - RED and PRO techniques, simply because it is able to work with extremely concentrated solutions of NaI or LiBr. By comparison, RED is limited to solutions with a boiling point elevation of 2-4 K, while the CRFB discussed in Ref. [76] works with solutions with a boiling point elevation of 45 K.

Efficiency η_{TS} increases with increasing solution concentration. CRFBs are needed to exploit highly concentrated solutions with a high η_{SGP} . The efficiency, up to 4%, is the highest reported in this paper.

Temperatures ΔT_* corresponds to the boiling point elevation of the solutions. A single effect distiller working with a large boiling point elevation, e.g. 45 K for LiBr aqueous solutions, works better than a multi-effect distiller working with small boiling point elevations, e.g. 2 K with NaCl.

MEHRS The higher is the boiling point elevation, the smaller is the size of the needed heat exchangers. High concentration solutions, handled by CRFBs, require a single-effect distiller (no MEHRS).

Power p of the order of $1 \text{ W}/\text{m}^2$ are obtained with RED; p of the order of $10 \text{ W}/\text{m}^2$ are achieved with PRO and CRFB. The latter have the possibility of further improvements, by development of suitable solid-state membranes.

Level of development The SGP processes have been realised in laboratory. VD and MD are industrially well developed. The integration of SGP with the TS has not been studied experimentally.

Overall remarks VD-CRFB appears as the most promising technique among the reviewed papers.

6.6.2 Membrane distillation (MD)

MD has the advantage of being compact, compared to VD. The efficiency is typically smaller than in VD, due to the heat conduction through the membrane [110, 81]. On the other hand, the physical process, vaporisation, is the same in VD and MD. The boiling point elevation, which plays a relevant role in VD, corresponds to the “threshold temperature” in MD, and the heat transferred as vaporisation latent heat is the same. It is thus expected that the performances of MD are rigorously lower than the performances of VD, due to the additional heat conduction which contributes to entropy production. Also in the case of MD, it has been noticed that a concentration increase has a positive effect on TS efficiency η_{TS} , although, with RED, such solutions would require “highly-performing membranes” [84] which are not yet available.

However, the studies of MD in the context of MD-SGP applications did not cover the very high concentrations that are the most promising for the TS-SGP techniques, such as the solutions used in VD-CRFBs. At this stage, it is thus impossible to conclude if MD is viable in a TS-SGP system: an evaluation of MD-SGP with high concentration solutions is needed.

6.6.3 Thermolysis (TL)

From Figs. 8 and 12, the TL-SGP techniques do not appear promising. However, as in the case of TRAB, the analysis of η_{TS} should rely on the evaluation of the column distillation techniques in the context of TS-SGP, which is still missing. The papers highlight that “future IEMs” [87], i.e. hypothetical future membranes with improved properties, could improve the performances.

Efficiency is quite small, of the order of 0.1%.

Temperatures T_H is around 70-80°C.

MEHRS Heat exchangers are used in the distillation column. Association in series of distillation columns has been proposed.

Power p is quite small, up to 1 W/m².

Level of development The SGP techniques have been experimentally tested in laboratory. TL is based on column distillation, which is well developed at industrial level. The experimental integration of TL with RED has been tested resulting in unsatisfactory results.

Overall remarks The current results do not appear promising, however, a fundamental understanding of the limitation of the technique is still missing, so it is not clear if significant improvements are still possible.

7 Conclusion

In this review we proposed a uniform framework for comparing the performances reported in literature for different innovative techniques for the exploitation of

low-temperature heat sources. The main parameters identified as performance indices are the energy efficiency η and the power density p . In the top-left corner of the $\eta - p$ graph, Fig. 8, we find two techniques, VD-CRFB and CuACN.

The performance index η is however dependent on the use of MEHRS, which require heat exchangers. We thus introduced a third performance index, ρ , which quantifies how much power can be produced with a fixed surface of heat exchangers in the MEHRS. The discussion of the results reported in literature and the theoretical work done on this topic showed that there is a trade-off between η and ρ , depending on the parameters of the used MEHRS; however, large values of both η and ρ can be obtained only with a large η_* , which is the energy efficiency of the bare process (i.e. the process without any MEHRS). In turn, large η_* also require large ΔT_* , i.e. a large temperature difference driving the bare process (i.e. the process without any MEHRS), which should be larger than the temperature difference across the heat exchangers, so, practically, of the order of 10 K.

The placing of the various techniques in the $\eta_* - \Delta T_*$ graph is shown in Fig. 12. Also in this case, two techniques are close to the top-right corner: VD-CRFB and CuACN. Actually, the use of the MEHRS enhances the performances of the techniques but it does not change the ranking, indeed techniques with large η_* (the top part of Fig. 12) also have a large η (top part of Fig. 8). Moreover, such techniques do not only yield a large η , but also require less heat exchangers in MEHRS: CuACN and VD-CRFB do not require MEHRS, and have larger efficiency than VD-RED techniques requiring 10 or 20 distiller effects.

Two key requirements are identified, in order to get a large η_* :

1. ΔT_* must be large, compatibly with $T_H < 100^\circ\text{C}$. The (single, no MEHRS) process must capture heat at high temperature from the heat source and releases it at much lower temperature to the heat sink.
2. The sensible heat exchanged during the cycle must be small (possibly, negligible) with respect to the heat reaction/latent heat captured from the heat source.

These two requirements can be graphically expressed by the temperature *versus* entropy graph. This tool is well known in the field of heat engines but can be applied also in our context. The former requirement says that the graph must show an almost horizontal upper segment, representing the capture from the heat source, and an almost horizontal lower segment, representing the release of heat to the heat source, spaced by a large ΔT_* . The latter requirement says that the conjunction between the two almost horizontal segments must be as vertical as possible, compared to the overall width of the graph, i.e. the cycle must approach a rectangle, the Carnot cycle.

The two requirements explain the placing of the various techniques. In CuACN and VD-SGP, the sensible heat exchange is negligible with respect to the reaction and vaporisation heat, hence they show good performances. In distillation-based techniques, ΔT_* is the boiling point elevation of the solution.

When RED is used, the concentration is at most a few molar, the boiling point elevation is limited to a few K, and thus the efficiency is small. Instead, the VD-CRFB work at much higher concentrations, thus the much larger overall efficiency η that is reached.

In TREC, the reaction heat is much smaller than in CuACN and VD-SGP. For this reason, the sensible heat exchange comes significantly into play. Currently, the experiments did not yet demonstrate the feasibility of cells with a large ratio between reaction and sensible heat, so the efficiency reported in Fig. 8 is only theoretical.

Our analysis identifies two promising research lines:

1. CuACN technique uses a heat-driven chemical reaction as regeneration stage. The reaction heat is large and the reaction takes place at a large ΔT_* . Besides research for increasing the TRL of the technique, alternative chemistries could be studied. Regeneration by means of chemical reactions typically take place at high temperature ($> 100^\circ\text{C}$) [54]; the challenge is to find reactions taking place at lower temperature.
2. VD-RFB exploits the vaporisation to capture heat from the heat source. The vaporisation latent heat is larger than the sensible heat, in the considered temperature range. Alternative SGP techniques working at very high concentrations could be studied in order to improve even more the performances and reach higher TRL.

In order to unify future research in this field, we suggest that a paper should report the following data:

1. Placing of the technique in the $\eta - p$ graph and comparison with competing techniques;
2. Placing of the technique in the $\eta_* - \Delta T_*$ graph and comparison with competing techniques;
3. Discussion of the limits of the technique: what are the theoretical limits? Why they are not reached in the experiments? What can be done in order to increase the performances?
4. When possible, the energy efficiency should be discussed showing a temperature *versus* entropy graph.

All the parameters should be given homogeneously, e.g. the power densities should be compared with literature results using the same normalisation (for example, power per unit membrane area). The performance indices should be evaluated at the same working conditions, giving (a set of) η with the corresponding p ; it is of little use to report the maximum power density p if it is obtained at a vanishingly small η . If MEHRS are used, η must be compared with literature results at same ΔT_{he} . In order to compare the results with Fig. 12, the performance indices must be reported with $\Delta T_{he}=5$ K.

Conflicts of interest

There are no conflicts of interest to declare.

References

- [1] I. Müller, *A History of Thermodynamics - The Doctrine of Energy and Entropy*, Springer, Berlin, 2006.
- [2] J. Ghojel, *Fundamentals of Heat Engines*, John Wiley & Sons Ltd, Hoboken, NJ, 2020. doi:10.1002/9781119548829.
- [3] H. Chen, D. Y. Goswami, E. K. Stefanakos, A review of thermodynamic cycles and working fluids for the conversion of low-grade heat, *Renewable and Sustainable Energy Reviews* 14 (2010) 3059–3067. doi:10.1016/j.rser.2010.07.006.
- [4] S. Chu, A. Majumdar, Opportunities and challenges for a sustainable energy future, *Nature* 488 (7411) (2012) 294–303. doi:10.1038/nature11475.
- [5] D. Mills, Advances in solar thermal electricity technology, *Solar Energy* 76 (1–3) (2004) 19–31. doi:10.1016/S0038-092X(03)00102-6.
- [6] T. Tartière, M. Astolfi, A world overview of the organic rankine cycle market, *Energy Procedia* 129 (2017) 2–9. doi:10.1016/j.egypro.2017.09.159.
- [7] European energy security strategy, accessed on 25/08/2020 (2014). URL <https://ec.europa.eu/energy/topics/energy-strategy/previous-energy-strategies>
- [8] S. Pfenninger, P. Gauché, J. Lilliestam, K. Damerau, F. Wagner, A. Patt, Potential for concentrating solar power to provide baseload and dispatchable power, *Nature Climate Change* 4 (2014) 689–692. doi:10.1038/nclimate2276.
- [9] Y. Tian, C. Y. Zhao, A review of solar collectors and thermal energy storage in solar thermal applications, *Applied Energy* 104 (2013) 538–553. doi:10.1016/j.apenergy.2012.11.051.
- [10] P. Bermel, K. Yazawa, J. L. Gray, X. Xu, A. Shakouri, Hybrid strategies and technologies for full spectrum solar conversion, *Energy & Environmental Science* 9 (9) (2016) 2776–2788. doi:10.1039/c6ee01386d.
- [11] F. Cao, K. McEnaney, G. Chen, Z. F. Ren, A review of cermet-based spectrally selective solar absorbers, *Energy & Environmental Science* 7 (5) (2014) 1615–1627. doi:10.1039/c3ee43825b.

- [12] A. R. Mazhar, S. Liu, A. Shukla, A state of art review on district heating systems, *Renewable and Sustainable Energy Reviews* 96 (2018) 420–439. doi:10.1016/j.rser.2018.08.005.
- [13] M. De Paepe, P. D’Herdt, D. Mertens, Micro-chp systems for residential applications, *Energy Conversion and Management* 47 (18–19) (2006) 3435–3446. doi:10.1016/j.enconman.2005.12.024.
- [14] R. DiPippo, *Geothermal power plants, third edition Edition*, Butterworth-Heinemann, Oxford, 2012.
- [15] E. Barbier, Geothermal energy technology and current status: an overview, *Renewable & Sustainable Energy Reviews* 6 (1–2) (2002) 3–65. doi:10.1016/S1364-0321(02)00002-3.
- [16] C. Forman, I. K. Muritala, R. Pardemann, B. Meyer, Estimating the global waste heat potential, *Renewable & Sustainable Energy Reviews* 57 (2016) 1568–1579. doi:10.1016/j.rser.2015.12.192.
- [17] I. Johnson, T. William, W. Choate, A. Davidson, *Waste heat recovery: technology and opportunities in us industry*, uS Department of Energy, office of energy efficiency and renewable energy, Industrial Technologies Program (2008). doi:10.2172/1218716.
- [18] F. Campana, M. Bianchi, L. Branchini, A. D. Pascale, A. Peretto, M. Baresi, A. Fermi, N. Rossetti, R. Vescovo, ORC waste heat recovery in European energy intensive industries: Energy and GHG savings, *Energy Conversion and Management* 76 (2013) 244–252. doi:10.1016/j.enconman.2013.07.041.
- [19] WiseGRID, accessed on 25/08/2020 (2020). URL <https://www.wisegrid.eu>
- [20] I. Tlili, Y. Timoumi, S. Ben Nasrallah, Analysis and design consideration of mean temperature differential stirling engine for solar application, *Renew. Energ.* 33 (8) (2008) 1911–1921. doi:10.1016/j.renene.2007.09.024.
- [21] T. Hung, T. Y. Shai, S. K. Wang, A review of organic rankine cycles (ORCs) for the recovery of low-grade waste heat, *Energy* 22 (7) (1997) 661–667. doi:10.1016/S0360-5442(96)00165-X.
- [22] L. E. Bell, Cooling, heating, generating power, and recovering waste heat with thermoelectric systems, *Science* 321 (5895) (2008) 1457–1461. doi:10.1126/science.1158899.
- [23] M. Rahimi, A. P. Straub, F. Zhang, X. Zhu, M. Elimelech, C. A. Gorski, B. E. Logan, Emerging electrochemical and membrane-based systems to convert low-grade heat to electricity, *Energy & Environmental Science* 11 (2) (2018) 276–285. doi:10.1039/c7ee03026f.

- [24] O. K. Singh, S. C. Kaushik, Thermo-economic evaluation and optimization of a Brayton–Rankine–Kalina combined triple power cycle, *Energy Conversion and Management* 71 (2013) 32–42. doi:10.1016/j.enconman.2013.03.017.
- [25] K. Mistry, M. A. Antar, J. H. Lienhard V, An improved model for multiple effect distillation, *Desalination and Water Treatment* 51 (2013) 807–821. doi:10.1080/19443994.2012.703383.
- [26] S. W. Lee, Y. Yang, H.-W. Lee, H. Ghasemi, D. Kraemer, G. Chen, Y. Cui, An electrochemical system for efficiently harvesting low-grade heat energy, *Nature Communications* 5 (2014) 3942. doi:10.1038/ncomms4942.
- [27] Y. Yang, J. Loomis, H. Ghasemi, S. W. Lee, Y. J. Wang, Y. Cui, G. Chen, Membrane-free battery for harvesting low-grade thermal energy, *Nano Lett.* 14 (2014) 6578. doi:10.1021/nl5032106.
- [28] Y. Yang, S. W. Lee, H. Ghasemi, J. Loomis, X. Li, D. Kraemer, G. Zheng, Y. Cui, G. Chen, Charging-free electrochemical system for harvesting low-grade thermal energy, *Proc. Natl. Acad. Sci. U. S. A.* 111 (2014) 17011. doi:10.1073/pnas.1415097111.
- [29] R. H. Hammond, W. M. Risen, An electrochemical heat engine for direct solar energy conversion, *Solar Energy* 23 (1979) 443–449. doi:10.1016/0038-092X(79)90153-1.
- [30] X. Wang, Y.-T. Huang, C. Liu, K. Mu, K. H. Li, S. Wang, C.-H. Su, S.-P. Feng, Direct thermal charging cell for converting low-grade heat to electricity, *Nature Communications* 10 (2019) 4151–4158. doi:10.1038/s41467-019-12144-2.
- [31] A. D. Poletayev, I. S. McKay, W. C. Chueh, A. Majumdar, Continuous electrochemical heat engines, *Energy Environ. Sci.* 11 (2018) 2964–2971. doi:10.1039/c8ee01137k.
- [32] S. Ahualli, M. M. Fernandez, G. Iglesias, A. V. Delgado, L. L. Jimenez, Temperature effects on energy production by salinity exchange, *Environ. Sci. Tech.* 48 (20) (2014) 12378–12385. doi:10.1021/es500634f.
- [33] B. B. Sales, O. S. Burheim, S. Porada, V. Presser, C. J. N. Buisman, H. V. M. Hamelers, Extraction of energy from small thermal differences near room temperature using capacitive membrane technology, *Environ. Sci. Technol. Lett.* 1 (9) (2014) 356–360. doi:10.1021/ez5002402.
- [34] A. Härtel, M. Janssen, D. Weingarh, V. Presser, R. van Rooij, Heat-to-current conversion of low-grade heat from a thermocapacitive cycle by supercapacitors, *Energy Environ. Sci.* 8 (8) (2015) 2396–2401. doi:10.1039/c5ee01192b.

- [35] P. Peljo, D. Lloyd, D. Nguyet, M. Majaneva, K. Kontturi, Towards a thermally regenerative all-copper redox flow battery, *Phys. Chem. Chem. Phys.* 16 (2014) 2831–2835. doi:10.1039/c3cp54585g.
- [36] S. Maye, H. H. Girault, P. Peljo, Thermally regenerative copper nanoslurry flow batteries for heat-to-power conversion with low-grade thermal energy, *Energy & Environmental Science* (2020). doi:10.1039/DOEE01590C.
- [37] F. Zhang, J. Liu, W. Yang, B. E. Logan, A thermally regenerative ammonia-based battery for efficient harvesting of low-grade thermal energy as electrical power, *Energ. Environ. Sci.* 8 (2015) 343–349. doi:10.1039/C4EE02824D.
- [38] F. Zhang, N. La Barge, W. Yang, J. Liu, B. E. Logan, Enhancing low-grade thermal energy recovery in a thermally regenerative ammonia battery using elevated temperatures, *ChemSusChem* 8 (6) (2015) 1043–1048. doi:10.1002/cssc.201403290.
- [39] X. Zhu, M. Rahimi, C. A. Gorski, B. Logan, A thermally-regenerative ammonia-based flow battery for electrical energy recovery from waste heat, *ChemSusChem* 9 (8) (2016) 873–9. doi:10.1002/cssc.201501513.
- [40] H. Tian, W. Jiang, G. Q. Shu, W. G. Wang, D. X. Huo, M. Z. Shakir, Analysis and optimization of thermally-regenerative ammonia-based flow battery based on a 3-d model, *J. Electrochem. Soc.* 166 (13) (2019) A2814–A2825. doi:10.1149/2.0711912jes.
- [41] M. Rahimi, A. D’Angelo, C. A. Gorski, O. Scialdone, B. E. Logan, Electrical power production from low-grade waste heat using a thermally regenerative ethylenediamine battery, *J. Power Sources* 351 (2017) 45–50. doi:10.1016/j.jpowsour.2017.03.074.
- [42] M. Rahimi, T. Kim, C. A. Gorski, B. E. Logan, A thermally regenerative ammonia battery with carbon-silver electrodes for converting low-grade waste heat to electricity, *Journal of Power Sources* 373 (2018) 95–102. doi:10.1016/j.jpowsour.2017.10.089.
- [43] W. G. Wang, G. Q. Shu, H. Tian, D. X. Huo, X. P. Zhu, A bimetallic thermally-regenerative ammonia-based flow battery for low-grade waste heat recovery, *J. Power Sources* 424 (2019) 184–192. doi:10.1016/j.jpowsour.2019.03.086.
- [44] W. G. Wang, H. Tian, G. Q. Shu, D. X. Huo, F. Zhang, X. P. Zhu, A bimetallic thermally regenerative ammonia-based battery for high power density and efficiently harvesting low-grade thermal energy, *J. Mat. Chem. A* 7 (11) (2019) 5991–6000. doi:10.1039/c8ta10257k.

- [45] A. P. Straub, N. Y. Yip, S. H. Lin, J. Lee, M. Elimelech, Harvesting low-grade heat energy using thermo-osmotic vapour transport through nanoporous membranes, *Nature Energy* 1 (2016) 16090. doi:10.1038/NENERGY.2016.90.
- [46] A. P. Straub, M. Elimelech, Energy efficiency and performance limiting effects in thermo-osmotic energy conversion from low-grade heat, *Environ. Sci. Technol.* 51 (21) (2017) 12925–12937. doi:10.1021/acs.est.7b02213.
- [47] X. Chen, C. Boo, N. Y. Yip, Low-temperature heat utilization with vapor pressure-driven osmosis: Impact of membrane properties on mass and heat transfer, *J. Membr. Sci.* 588 (2019) 117181. doi:10.1016/j.memsci.2019.117181.
- [48] Z. W. Yuan, Y. X. Yu, L. Wei, X. Sui, Q. H. She, Y. Chen, Pressure-retarded membrane distillation for simultaneous hypersaline brine desalination and low-grade heat harvesting, *J. Membr. Sci.* 597 (2020) 117765. doi:10.1016/j.memsci.2019.117765.
- [49] X. K. Liu, L. S. Shu, S. P. Jin, A modeling investigation on the thermal effect in osmosis with gap-filled vertically aligned carbon nanotube membranes, *J. Membr. Sci.* 580 (2019) 143–153. doi:10.1016/j.memsci.2019.03.002.
- [50] Z. W. Yuan, L. Wei, J. D. Afroz, K. Goh, Y. M. Chen, Y. X. Yu, Q. H. She, Y. Chen, Pressure-retarded membrane distillation for low-grade heat recovery: The critical roles of pressure-induced membrane deformation, *J. Membr. Sci.* 579 (2019) 90–101. doi:10.1016/j.memsci.2019.02.045.
- [51] L. Fu, S. Merabia, L. Joly, Understanding fast and robust thermo-osmotic flows through carbon nanotube membranes: Thermodynamics meets hydrodynamics, *J. Phys. Chem. Letters* 9 (8) (2018) 2086–2092. doi:10.1021/acs.jpcllett.8b00703.
- [52] K. Park, D. Y. Kim, D. R. Yang, Theoretical analysis of pressure retarded membrane distillation (PRMD) process for simultaneous production of water and electricity, *Industrial & Engineering Chemistry Research* 56 (50) (2017) 14888–14901. doi:10.1021/acs.iecr.7b03642.
- [53] D. W. Gerlach, T. A. Newell, Basic modelling of direct electrochemical cooling, *Int. J. Energy Res.* 31 (2007) 439–454. doi:10.1002/er.1250.
- [54] H. L. Chum, R. Osteryoung, Review of thermally regenerative electrochemical systems, accessed on 16/02/2017 (1980-81). URL http://www.nrel.gov/docs/legosti/old/416_v1.pdf
- [55] T. I. Quickenden, Y. Mua, A review of power generation in aqueous thermogalvanic cells, *J. Electrochem. Soc.* 142 (11) (1995) 3985–3994.

- [56] T. I. Quickenden, C. F. Vernon, Thermogalvanic conversion of heat to electricity, *Solar Energy* 36 (1) (1986) 63–72. doi:10.1016/0038-092X(86)90061-7.
- [57] M. F. Dupont, D. R. MacFarlane, J. M. Pringle, Thermo-electrochemical cells for waste heat harvesting – progress and perspectives, *Chem. Commun.* 53 (2017) 6288–6302. doi:10.1039/C7CC02160G.
- [58] C. Gao, S. W. Lee, Y. Yang, Thermally regenerative electrochemical cycle for low-grade heat harvesting, *ACS Energy Lett.* 2 (10) (2017) 2326–2334. doi:10.1021/acsenergylett.7b00568.
- [59] D. Brogioli, Extracting renewable energy from a salinity difference using a capacitor, *Phys. Rev. Lett.* 103 (2009) 058501.
- [60] F. La Mantia, M. Pasta, H. D. Deshazer, B. E. Logan, Y. Cui, Batteries for efficient energy extraction from a water salinity difference, *Nano Lett.* 11 (2011) 1810–1813. doi:10.1021/nl200500s.
- [61] R. H. Hammond, W. M. Risen, An electrochemical heat engine for direct solar energy conversion, *Solar Energy* 23 (1979) 443–449. doi:10.1016/0038-092X(79)90153-1.
- [62] A. J. Bard, L. R. Faulkner, Double-layer structure and adsorbed intermediates in electrode processes, *J. Wiley and sons*, New York, 1980, Ch. 12, pp. 488–515.
- [63] L. C. Moulthrop, T. M. Molter, A. J. Speranza, M. A. Lillis, W. Smith, J. Shiepe, T. M. Skoczylas, Regenerative electrochemical cell system and method for use thereof, patent US2005129996 (2005).
- [64] R. Long, Y. A. Zhao, Z. Q. Luo, L. Li, Z. C. Liu, W. Liu, Alternative thermal regenerative osmotic heat engines for low-grade heat harvesting, *Energy* 195 (2020) 117042. doi:10.1016/j.energy.2020.117042.
- [65] T. Thorsen, T. Holt, The potential for power production from salinity gradients by pressure retarded osmosis, *J. Membr. Sci.* 335 (1–2) (2009) 103–110. doi:10.1016/j.memsci.2009.03.003.
- [66] A. Altaee, P. Palenzuela, G. Zaragoza, A. A. AlAnezi, Single and dual stage closed-loop pressure retarded osmosis for power generation: Feasibility and performance, *Applied Energy* 191 (2017) 328–345. doi:10.1016/j.apenergy.2017.01.073.
- [67] F. Giacalone, C. Olkis, G. Santori, A. Cipollina, S. Brandani, G. Micale, Novel solutions for closed-loop reverse electrodialysis: Thermodynamic characterisation and perspective analysis, *Energy* 166 (2019) 674–689. doi:10.1016/j.energy.2018.10.049.

- [68] B. Ortega-Delgado, F. Giacalone, P. Catrini, A. Cipollina, A. Piacentino, A. Tamburini, G. Micale, Reverse electro dialysis heat engine with multi-effect distillation: Exergy analysis and perspectives, *Energy Conversion and Management* 194 (2019) 140–159. doi:10.1016/j.enconman.2019.04.056.
- [69] B. Ortega-Delgado, F. Giacalone, A. Cipollina, M. Papapetrou, G. Kosmadakis, A. Tamburini, G. Micale, Boosting the performance of a reverse electro dialysis - multi-effect distillation heat engine by novel solutions and operating conditions, *Appl. Energy* 253 (2019) 113489. doi:10.1016/j.apenergy.2019.113489.
- [70] P. Palenzuela, M. Micari, B. Ortega-Delgado, F. Giacalone, G. Zaragoza, D. C. Alarcon-Padilla, A. Cipollina, A. Tamburini, G. Micale, Performance analysis of a RED-MED salinity gradient heat engine, *Energies* 11 (12) (2018) 3385. doi:10.3390/en11123385.
- [71] M. Papapetrou, G. Kosmadakis, F. Giacalone, B. Ortega-Delgado, A. Cipollina, A. Tamburini, G. Micale, Evaluation of the economic and environmental performance of low-temperature heat to power conversion using a reverse electro dialysis - multi-effect distillation system, *Energies* 12 (17) (2019). doi:10.3390/en12173206.
- [72] A. Tamburini, M. Tedesco, A. Cipollina, G. Micale, M. Ciofalo, M. Papapetrou, W. Van Baak, A. Piacentino, Reverse electro dialysis heat engine for sustainable power production, *Applied Energy* 206 (2017) 1334–1353. doi:10.1016/j.apenergy.2017.10.008.
- [73] M. Marino, L. Misuri, A. Carati, D. Brogioli, Proof-of-concept of a zinc-silver battery for the extraction of energy from a concentration difference, *Energies* 7 (6) (2014) 3664–3683. doi:10.3390/en7063664.
- [74] M. Marino, L. Misuri, A. Carati, D. Brogioli, Boosting the voltage of a salinity-gradient-power electrochemical cell by means of complex-forming solutions, *Appl. Phys. Lett.* 105 (2014) 033901. doi:10.1063/1.4890976.
- [75] I. Facchinetti, R. Ruffo, F. La Mantia, D. Brogioli, Thermally-regenerable redox flow battery for exploiting low-temperature heat sources, *Cell Reports Physical Science* 1 (5) (2020) 100056. doi:10.1016/j.xcrp.2020.100056.
- [76] I. Facchinetti, E. Cobani, D. Brogioli, F. La Mantia, R. Ruffo, Thermally regenerable redox flow battery, *ChemSusChem* 13 (2020) 5460–5467. doi:10.1002/cssc.202001799.
- [77] A. Carati, M. Marino, D. Brogioli, Thermodynamic study of a distiller-electrochemical cell system for energy production from low temperature heat sources, *Energy* 93 (1) (2015) 984–993. doi:10.1016/j.energy.2015.09.108.

- [78] D. Brogioli, F. La Mantia, N. Y. Yip, Thermodynamic analysis and energy efficiency of thermal desalination processes, *Desalination* 428 (2018) 29–39. doi:10.1016/j.desal.2017.11.010.
- [79] D. Brogioli, F. La Mantia, N. Y. Yip, Energy efficiency analysis of distillation for thermally regenerative salinity gradient power technologies, *Renewable Energy* 133 (2019) 1034–1045. doi:10.1016/j.renene.2018.10.107.
- [80] K. L. Hickenbottom, J. Vanneste, L. Miller-Robbie, A. Deshmukh, M. Elimelech, M. B. Heeley, T. Y. Cath, Techno-economic assessment of a closed-loop osmotic heat engine, *Journal of Membrane Science* 535 (2017) 178–187. doi:10.1016/j.memsci.2017.04.034.
- [81] S. H. Lin, N. Y. Yip, T. Y. Cath, C. O. Osuji, M. Elimelech, Hybrid pressure retarded osmosis-membrane distillation system for power generation from low-grade heat: thermodynamic analysis and energy efficiency, *Environ. Sci. Technol.* 48 (9) (2014) 5306–5313. doi:10.1021/es405173b.
- [82] E. Shaulsky, C. Boo, S. H. Lin, M. Elimelech, Membrane-based osmotic heat engine with organic solvent for enhanced power generation from low-grade heat, *Environ. Sci. Technol.* 49 (9) (2015) 5820–5827. doi:10.1021/es506347j.
- [83] R. Long, B. Li, Z. Liu, W. Liu, Hybrid membrane distillation-reverse electro dialysis electricity generation system to harvest low-grade thermal energy, *J. Memb. Sci.* 525 (2017) 107–115. doi:10.1016/j.memsci.2016.10.035.
- [84] M. Micari, A. Cipollina, F. Giacalone, G. Kosmadakis, M. Papapetrou, G. Zaragoza, G. Micale, A. Tamburini, Towards the first proof of the concept of a reverse electro dialysis - membrane distillation heat engine, *Desalination* 453 (2019) 77–88. doi:10.1016/j.desal.2018.11.022.
- [85] R. L. McGinnis, J. R. McCutcheon, M. Elimelech, A novel ammonia-carbon dioxide osmotic heat engine for power generation, *J. Membr. Sci.* 305 (1–2) (2007) 13–19. doi:10.1016/j.memsci.2007.08.027.
- [86] M. Bevacqua, A. Tamburini, M. Papapetrou, A. Cipollina, G. Micale, A. Piacentino, Reverse electro dialysis with NH_4HCO_3 -water systems for heat-to-power conversion, *Energy* 137 (2017) 1293–1307. doi:10.1016/J.ENERGY.2017.07.012.
- [87] F. Giacalone, F. Vassallo, L. Griffin, M. C. Ferrari, G. Micale, F. Scargiali, A. Tamburini, A. Cipollina, Thermolytic reverse electro dialysis heat engine: model development, integration and performance analysis, *Energy Conversion and Management* 189 (2019) 1–13. doi:10.1016/j.enconman.2019.03.045.

- [88] F. Giacalone, F. Vassallo, F. Scargiali, A. Tamburini, A. Cipollina, G. Micale, The first operating thermolytic reverse electro dialysis heat engine, *J. Membr. Sci.* 595 (2020) 117522. doi:10.1016/j.memsci.2019.117522.
- [89] M. C. Hatzell, B. E. Logan, Evaluation of flow fields on bubble removal and system performance in an ammonium bicarbonate reverse electro dialysis stack, *J. Membr. Sci.* 446 (2013) 449–455. doi:10.1016/j.memsci.2013.06.019.
- [90] M. C. Hatzell, I. Ivanov, R. D. Cusick, X. P. Zhu, B. E. Logan, Comparison of hydrogen production and electrical power generation for energy capture in closed-loop ammonium bicarbonate reverse electro dialysis systems, *Phys. Chem. Chem. Phys.* 16 (4) (2014) 1632–1638. doi:10.1039/c3cp54351j.
- [91] D. H. Kim, B. H. Park, K. Kwon, L. Li, D. Kim, Modeling of power generation with thermolytic reverse electro dialysis for low-grade waste heat recovery, *Applied Energy* 189 (2017) 201–210. doi:10.1016/j.apenergy.2016.10.060.
- [92] K. Kwon, B. H. Park, D. H. Kim, D. Kim, Parametric study of reverse electro dialysis using ammonium bicarbonate solution for low-grade waste heat recovery, *Energy Conversion and Management* 103 (2015) 104–110. doi:10.1016/j.enconman.2015.06.051.
- [93] X. Luo, X. Cao, Y. Mo, K. Xiao, X. Zhang, P. Liang, X. Huang, Power generation by coupling reverse electro dialysis and ammonium bicarbonate: Implication for recovery of waste heat, *Electrochem. Comm.* 19 (2012) 25–28. doi:10.1016/j.elecom.2012.03.004.
- [94] R. D. Cusick, Y. Kim, B. E. Logan, Energy capture from thermolytic solutions in microbial reverse-electro dialysis cells, *Science* 335 (6075) (2012) 1474–1477. doi:10.1126/science.1219330.
- [95] J. Y. Nam, R. D. Cusick, Y. Kim, B. E. Logan, Hydrogen generation in microbial reverse-electro dialysis electrolysis cells using a heat-regenerated salt solution, *Environ. Sci. Technol.* 46 (2012) 5240–5246. doi:10.1021/es300228m.
- [96] T. Kim, M. Rahimi, B. E. Logan, C. Gorski, Evaluating battery-like reactions to harvest energy from salinity differences using ammonium bicarbonate salt solutions, *ChemSusChem* 9 (9) (2016) 981–988. doi:10.1002/cssc.201501669.
- [97] Y. Zhong, X. Wang, X. Feng, S. Telalovic, Y. Gnanou, K.-W. Huang, X. Hu, Z. Lai, Osmotic heat engine using thermally responsive ionic liquids, *Environ. Sci. Technol.* 51 (16) (2017) 9403–9409. doi:10.1021/acs.est.7b02558.

- [98] V. Styliaras, Electric energy production by voltaic cell solution temperature change, patent WO 2008059297 A1, 2008 (2008).
- [99] D. Anastasio, J. T. Arena, E. A. Cole, J. R. McCutcheon, Impact of temperature on power density in closed-loop pressure retarded osmosis for grid storage, *Journal of Membrane Science* 479 (2015) 240–245. doi:10.1016/j.memsci.2014.12.046.
- [100] M. Micari, M. Bevacqua, A. Cipollina, A. Tamburini, W. Van Baak, T. Putts, G. Micale, Effect of different aqueous solutions of pure salts and salt mixtures in reverse electrodialysis systems for closed-loop applications, *J. Membr. Sci.* 551 (2018) 315–325. doi:10.1016/j.memsci.2018.01.036.
- [101] X. Zhu, W. He, B. E. Logan, Influence of solution concentration and salt types on the performance of reverse electrodialysis cells, *Journal of Membrane Science* 494 (2015) 154–160. doi:10.1016/j.memsci.2015.07.053.
- [102] A. D. Khawaji, I. K. Kutubkhanah, J. M. Wie, Advances in seawater desalination technologies, *Desalination* 221 (1–3) (2008) 47–69. doi:10.1016/j.desal.2007.01.067.
- [103] A. M. Alklaibi, N. Lior, Membrane-distillation desalination: Status and potential, *Desalination* 171 (2) (2005) 111–131. doi:10.1016/j.desal.2004.03.024.
- [104] R. K. Sinnott, *Coulson & Richardson’s chemical engineering - Chemical Engineering Design*, 4th Edition, Vol. 6, Elsevier Butterworth Heinemann, Amsterdam, 2005.
- [105] J. D. Isaacs, R. J. Seymour, The ocean as a power resource, *International Journal of Environmental Studies* 4 (1973) 201–205. doi:10.1080/00207237308709563.
- [106] O. Levenspiel, N. de Vevers, The osmotic pump, *Science* 183 (1974) 157–160.
- [107] J. N. Weinstein, F. B. Leitz, Electric power from differences in salinity: the dialytic battery, *Science* 191 (1976) 557–559.
- [108] G. L. Soloveichik, Flow batteries: Current status and trends, *Chem. Rev.* 115 (20) (2015) 11533–11558. doi:10.1021/cr500720t.
- [109] C.-G. Han, X. Qian, Q. Li, B. Deng, Y. Zhu, Z. Han, W. Zhang, W. Wang, S.-P. Feng, G. Chen, W. Liu, Giant thermopower of ionic gelatin near room temperature, *Science* 368 (2020) 1091–1098. doi:10.1126/science.aaz5045.

- [110] S. Lin, N. Y. Yip, M. Elimelech, Direct contact membrane distillation with heat recovery: thermodynamic insights from module scale modeling, *J. Membr. Sci.* 453 (2014) 498–515.
- [111] D. Brogioli, F. L. Mantia, Heat recovery in energy production from low temperature heat sources, *AIChE Journal* 65 (2019) 980–991. doi:10.1002/aic.16496.
- [112] G. Kosmadakis, M. Papapetrou, B. Ortega-Delgado, A. Cipollina, D.-C. Alarcón-Padilla, Correlations for estimating the specific capital cost of multi-effect distillation plants considering the main design trends and operating conditions, *Desalination* 447 (2018) 74–83. doi:10.1016/j.desal.2018.09.011.
- [113] G. F. Hewitt, S. J. Pugh, Approximate design and costing methods for heat exchangers, *Heat Transfer Engineering* 28 (2) (2007) 76–86. doi:10.1080/01457630601023229.
- [114] P. Peljo, personal communication (2020).
- [115] M. Blahušiak, A. A. Kiss, S. R. A. Kersten, B. Schuur, Quick assessment of binary distillation efficiency using a heat engine perspective, *Energy* 116 (1) (2016) 20–31. doi:10.1016/j.energy.2016.09.097.
- [116] N. Y. Yip, M. Elimelech, Comparison of energy efficiency and power density in pressure retarded osmosis and reverse electro dialysis, *Environ. Sci. Technol.* 48 (18) (2014) 11002–11012. doi:10.1021/es5029316.